$$w_1(r_d)_S = 2r_d e^{-r_d^2 - r_{oa}^2} I_o(2r_{oa}r_d), \quad (r_d, r_{oa} \geq 0), \tag{3.4a}$$

or

$$w_1(\lambda)_S = \frac{2c_o^2}{\hat{r}_o^2} \lambda e^{-\lambda^2(c_o/\hat{r}_o)^2 - r_{oa}^2} I_o(2r_{oa}c_o\lambda/\hat{r}_o) , \quad (r_{oa}, \lambda > 0). \tag{3.4b}$$

When the source is not moving, but its location is unknown to the receiver, the pdf of its location can be usefully expressed alternatively by the density function [9],

$$w_1(\lambda)_S = B_\mu \lambda^{1-\mu} d\lambda w_1(\phi) d\phi \quad ; \quad B_\mu = \frac{2-\mu}{\lambda_1^{2-\mu} - \lambda_o^{2-\mu}} \; ; \; \left.\begin{array}{r} (0<)\lambda_o \leq \lambda_1 (<\infty) \\ 0 \leq \phi \leq 2\pi \end{array}\right\} , \; \mu \geq 0. \tag{3.5}$$

for the simple geometry of Figure 3.1, where the possible location of the source is in the region Λ_S. Other, more complex geometries may be handled in the same fashion, but this rather simple model often gives reasonable and representative results.

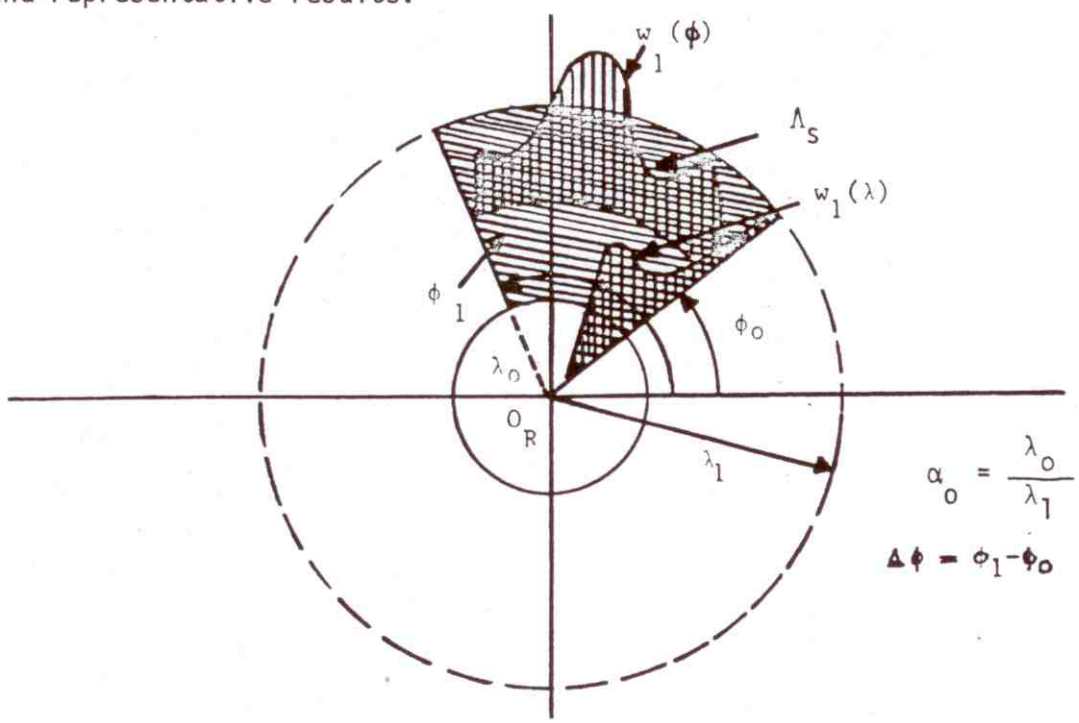

Figure 3.1. Schema of $w_1(\lambda)$, $w_1(\phi)$, Eq. (3.5); $\alpha_o (\equiv \lambda_o/\lambda_1)$ ratio of inner to outer radii.

3.2 EMI Scenarios: Calculation of Parameters:

The EMI scenario describes how a typical interfering source radiates and where it is located (statistically) in a domain (Λ_I) of such possible sources. It also provides an explicit structure for the resulting, typical waveform as seen following the linear front-end stages of the receiver. The scenario is fundamental in determining the explicit structure of the various distributions of the EMI itself, particularly when strictly canonical conditions do not hold, cf. [32], for Class A as well as Class B interference. Equally important, the EMI scenario allows us to calculate the principal parameters of these distributions, as we note below, cf. (3.10) ff.

The (first-order) EMI scenario is specifically defined by:

(3.6)

(i). the propagation law [$\lambda^{-\gamma}$, cf. (3.1a)], $\gamma>0$;

(ii). the distribution, σ_S, of sources in Λ_I; here $\sigma_S \sim \lambda^{-\mu} w_1(\phi)$;

(iii). the statistics of the fading parameter, $\underline{a}$, cf. (3.3),(3.1);

(iv). the average emission characteristics of the sources, as embodied in the "overlap index" A_A, A_B ;

(v). the structure of the wave-form-beam pattern factor

$$G_o(t,\phi)=|\mathcal{a}_{RT}(\phi)|\,b\,u_o(t,\underset{\sim}{\theta}') \ ,$$

cf. (2.17), [6]

where $\mathcal{a}_{RT}(\phi)$=composite source (T)-receiver (R) beam patterns,

u_o =normalized basic interference waveform in linear receiver output, before "processing";

b =appropriately dimensional parameter.

(vi). the statistics of any other pertinent parameters in the typical source model.

For the interfering sources we use (3.5) again, where Λ_I now is not necessarily the same domain as that for the desired signal source, Λ_S; Fig. 3.1 shows a typical domain. [We simplify without serious loss of

generality, by writing $\sigma_S(\lambda,\phi) = \sigma_s(\lambda)\sigma_S(\phi)$ here.] Note, for example, that $\mu=0$ corresponds to a uniform source distribution $\sigma_S(\lambda,\phi) = \sigma_{oS}/\lambda^{\mu} = \sigma_{oS}$. Specifically, the envelope of a typical source at the output of the front-end stages of the receiver (to the subsequent processing) is

$$\hat{B}_o = \frac{aG_o(\phi,t)}{\lambda^{\gamma}} \quad , \text{ cf. (3.1)} , \tag{3.7}$$

where now the scenario (3.6) applies.

The global, or "macro"-parameter of Class A, or Class B, interference are $\mathcal{P}_3 = \{A,\Omega_2,\Gamma'\}_{A,B}$, defined by

(3.8)
$A_{A,B}$ = "overlap index" = (av. no. of interfering sources emitting at any given instant) x (av. duration of a typical emission);

$\Omega_{2A,B} = [A\langle\hat{B}_o^2\rangle/2]_{A,B}$ = mean intensity of the nongaussian component of the EMI;

$\Gamma'_{A,B} \equiv [\sigma_G^2/\Omega_2]_{A,B}$ = gaussian factor, or ratio of the mean intensity of the gauss to the non-gauss component of the EMI;

$\bar{I}_N\big|_{A,B} = (\Omega_2+\sigma_G^2)_{A,B}$ = mean total intensity of the interference.

The gauss component is itself a sum of two components:

$$\sigma_G^2 = \sigma_E^2 + \sigma_R^2 , \tag{3.9}$$

the one due to (many) unresolvable external sources (σ_E^2), the other, to receiver noise, which appears largely in the initial (linear) stages of the receiver.

From (3.5)-(3.7) we can now readily calculate Ω_2,Γ', and $\bar{I}_N$. Thus, we have

$$\Omega_2 = A \frac{\overline{a^2}\langle G_o^2\rangle}{2} \frac{1}{\langle \lambda^{2\gamma}\rangle} \quad . \tag{3.10}$$

where $\langle G_o^2\rangle = \langle G_o^2\rangle_\phi$, etc., cf. (v), (3.6). From (3.5) it follows that

$$\langle 1/\lambda^{2\gamma}\rangle \equiv C_{\mu,\gamma}^{(2)} = \frac{2-\mu}{2\gamma+\mu-2}\left(\frac{1-\alpha_o^{2\gamma+\mu-2}}{1-\alpha_o^{2-\mu}}\right) \alpha_o^{2-2\gamma-\mu}\lambda_1^{-2\gamma} \; ; \; \alpha_o \equiv \lambda_o/\lambda_1 \tag{3.11}$$

with $(\mu,\gamma \geq 0)$. Similarly, Γ' and $\bar{I}_N$, cf. (3.8), become

$$\Gamma' = 2\sigma_G^2/A\, \overline{a^2}\, \overline{G_o^2}\, C_{\mu,\gamma}^{(2)} \; ; \; \bar{I}_N = A\, \overline{G_o^2}\, \frac{\overline{a^2}}{2}\, C_{\mu,\gamma}^{(2)} + \sigma_G^2 \; , \tag{3.12}$$

for Class A, or B interference. Clearly, the geometry and other elements of the EMI scenario strongly influence the magnitudes of these "macro"-parameters, cf. (3.8), and as we shall note below, the specific structure of the associated probability distributions.

Finally, we remark that more complex channel characteristics can be introduced, i.e. scatter channels which introduce spreading in frequency and path delay of both the desired signal and the interfering signals which may be developed along the lines of [3], [35], [36], and in a much more general way, by Middleton, in [37], [38]. For the 1st-order EMI's no correlation structures appear (we assume independent samples, or equivalently, noise samples taken outside the (rms) delay and frequency spread intervals). On the other hand, the correlation structure of the signal is preserved in our processing, so that the effects of channel "spread", if present, will modify the received signal. (We reserve the analysis to a later study.)

3.3 Probability Densities (of the Instantaneous Amplitudes):

It has been shown [32] that the EMI scenario can noticeably influence the form of the pdf (and APD) of Class A and B noise. We summarize the pertinent results established elsewhere (Class A, [32]; Class B, [5], [6]):

I. Class A Noise:

There are two principal developments for Class A interference [32]: (1), the "strictly canonical" forms, which correspond to source distributions where the potentially interfering sources are either equidistant, or approximately equidistant, from the receiver; and (2), the "quasi-canonical cases, where the sources are widely distributed in space and a or G_0 is rayleigh distributed. For the former we have the following expression for the first-order pdf (needed subsequently for locally optimum processing algorithms and performance, cf. Secs. 4-6):

(1). Strictly Canonical Class A pdf:

$$w_1(x)_{A+G} = e^{-A_A} \sum_{m=0}^{\infty} \frac{A_A^m}{m!} \frac{e^{-x^2/4\hat{\sigma}^2_{mA}}}{\sqrt{4\pi\hat{\sigma}^2_{mA}}} , \tag{3.13}$$

where

$$2\hat{\sigma}^2_{mA} \equiv \frac{m/A_A+\Gamma'_A}{1+\Gamma'_A} \quad ; \quad \Gamma'_A = \sigma_G^2/\Omega_{2A} \quad : \quad x = \frac{X}{\sqrt{\Omega_{2A}(1+\Gamma'_A)}} . \tag{3.13a}$$

Equation (3.13) is also appropriate for the "approximately" canonical cases, where the source distribution is no longer confined to sources equidistant from the receiver; [for details, see Sec. 5 of [32]].

(2). Quasi-Canonical Class A pdf:

$$w_1(x)_{A+G} \cong e^{-A_A \hat{g}_o} \sum_{m=0}^{\infty} \frac{(A_A \hat{g}_o)^m}{m!} \left\{ \frac{de^{-x^2 d^2/4\sigma^2_{om}}}{\sqrt{4\pi\sigma^2_{om}}} + \hat{\Phi}(0)(xd/2\sigma_{om}) \right\} , \tag{3.14}$$

where the "correction term" $\hat{\Phi}(0)$ is specifically

$$\hat{\Phi}(0) = \sum_{n=1}^{\infty} \frac{(-1)^n}{n!}\, {}_mC_n \cdot \frac{d}{\sqrt{4\pi\sigma_{om}^2}} \cdot \frac{\Gamma(1+\frac{n\alpha}{2})}{\sqrt{\pi}} \left[\frac{\pi}{2\Gamma(\frac{3+\alpha}{2})(m+\Gamma_A' A_A d^2)^{\alpha/2}}\right]^n$$

$$\cdot e^{-x^2 d^2/4\sigma_{om}^2}\, {}_1F_1(-\tfrac{n\alpha}{2}; 1/2; x^2 d^2/4\sigma_{om}^2) \ , \qquad (3.14a)$$

and where

$$2\sigma_{om}^2 \equiv \frac{m/A_A + \hat{\Gamma}_A}{1+\Gamma_A'} \ ; \ \hat{\Gamma}_A \equiv \Gamma_A' d^2 \ ; \ d^2\Big|_{\alpha_o<<1} \doteq \frac{\alpha}{2-\alpha} \cdot \frac{1}{\alpha_o^{(2-\alpha)\gamma}} \ (>>1) \qquad (3.14b)$$

$$(0<)\alpha = \frac{2-\mu}{\gamma} \ (<2) \ , \ \alpha_o \equiv \lambda_o/\lambda_1, \ {}_mC_n = \frac{m!}{(m-n)!n!} \ , \qquad (3.14c)$$

in which (μ,γ,α_o) are parameters of the EMI scenario, cf. Sec. (3.2) above, and $\hat{g}_o$ is a numerical scaling factor obtained by a suitably analytic "fitting" process, described in Secs. 7.2, 8.4 of [32].

For Class B interference we have, similarly ([6],[13],[33]):

II. Class B Noise:

Here we use a simplified version of the general first-order case [6], which involves only three parameters, instead of the usual six. Moreover, we assume a limiting form of the EMI scenario, where now α_o $(=\lambda_o/\lambda_1) \to 0$, e.g. $\lambda_o = 0$, cf. Fig. 3.1: potentially interfering sources can be effectively co-located with the receiver. This permits a considerable mathematical simplification of the resulting pdf [6] but, in turn, gives a distribution for which none of the moments exists (because the intensity at a point source is infinite, in such models). This defect is readily overcome in practice by truncating the pdf $w_1(x)$ at sufficiently large amplitudes $(x>>1)$, or equivalently, at sufficiently small values of the APD $(P_1 \equiv \int_{x_o}^{\infty} w_1(x)dx)$, [cf. Fig. 1, [33] and discussion therein]. [For the more complete model (still with $\lambda_o=0$, but suitably approximated at large x to insure finite moments, see [5],[6],[13].]

The appropriate pdf here is thus [from Eq. (2.10a), [13]], a

(3) (Quasi-Canonical Class B pdf ($\alpha_0 \to 0$):

$$w_1(x)_{B+G} \simeq \frac{e^{-x^2/\Omega_B}}{\pi\sqrt{\Omega_B}} \sum_{n=0}^{\infty} \frac{(-1)^n}{n!} \hat{A}_\alpha^n \, \Gamma(\tfrac{n\alpha+1}{2}) \; {}_1F_1(-\tfrac{n\alpha}{2}; 1/2; x^2/\Omega_B) \;, \qquad (3.15a)$$

or

$$\simeq \frac{1}{\pi\sqrt{\Omega_B}} \sum_{n=0}^{\infty} \frac{1}{n!} (-1)^n \hat{A}_\alpha^n \, \Gamma(\tfrac{n\alpha+1}{2}) \; {}_1F_1(\tfrac{1+n\alpha}{2}; 1/2; -x^2/\Omega_B) \;, \qquad (3.15b)$$

where α is given by (3.14c) and

$$\Omega_B \equiv 2\sqrt{2}\, G_B/N_I \;, \qquad (3.16a)$$

and

$$\hat{A}_\alpha = A_\alpha/2^\alpha G_B^\alpha = b_{1\alpha} A_B/[\tfrac{\Omega_{2B}}{2} \cdot (\tfrac{4-\alpha}{2-\alpha} + \Gamma_B')]^{\alpha/2} \;, \qquad (3.16b)$$

with

$$\left.\begin{aligned} A_\alpha &= 2^\alpha b_{1\alpha} A_B/[2\Omega_{2B}(1+\Gamma_B')]^{\alpha/2} \;;\; b_{1\alpha} = \frac{\Gamma(1-\frac{\alpha}{2})}{2^{\alpha/2}\Gamma(1+\frac{\alpha}{2})} \left\langle \left(\frac{\hat{B}_{oB}}{\sqrt{2}}\right)^\alpha \right\rangle \\ G_B^2 &\equiv (\tfrac{4-\alpha}{2-\alpha} + \Gamma_B')/4(1+\Gamma_B') \;. \end{aligned}\right\} \qquad (3.16c)$$

(It can be shown that $\int_{-\infty}^{\infty} w_1(x)_{A+G} dx = 1$, from the series development of ${}_1F_1$, etc., and moreover, that $w_1 \geq 0$, all x, as required of a proper pdf or directly from the characteristic function, (2.38), [6], with ($\lambda \to 0, \infty$) therein.) Thus, this model has three parameters $\mathcal{P}'_{3B} = \{\hat{A}_\alpha, \Omega_B, \alpha\}$. The parameter Ω_B is a normalizing parameter (through N_I in (3.16a), cf. (2.11c), [13]). As before, the "macro-parameters" $(A_B, \Omega_{2A}, \Gamma_B')$ are defined precisely as in the Class A cases, cf. (3.8). In practice, one uses a value of Ω_B which normalizes

the x-process to the measured intensity of the process, since the analytical second moment does not exist, for the reasons explained above. Although the more complete model ([6],[7],[13]) removes this difficulty, using (3.15a) in conjunction with empirical data does not at all limit the applicability of this simplified Class B model.

4. OPTIMUM* AND SUBOPTIMUM THRESHOLD DETECTION ALGORITHMS:

We now return to Section 2.2 above and consider both LOBD and selected suboptimum threshold detection algorithms, under the simplifying assumption of independent noise or interference samples. The correlated or "coherent" structure of the desired signal is, of course, preserved, since it is a critical element in enhancing the signal vis-à-vis the noise. For the suboptimum cases here we choose three types: I, correlation detectors, which are conventionally optimum when the noise or interference reduces to the gaussian; II, LOBD structures, where, however, there is a mismatch between the algorithm selected and the critical class of interference in which the desired signal is being received, or where the estimates of the noise parameters are noticeably imprecise, or both. And III, where correlation detectors (already suboptimum in nongaussian noise) are used in similar "mismatched" situations.

We begin with the optimum cases:

4.1 LOBD Detection Algorithms:

From (2.11)-(2.16) we obtain for independent (but not necessarily stationary) noise samples the following results

I. Coherent Reception (H_1 vs. H_0):

$$g(\underset{\sim}{x})^*_c = [\log \mu + \hat{B}^*_{n\text{-coh}}] - \sum_{j=1}^{n} \langle a_{oj} s_j \rangle \ell_j \ , \tag{4.1}$$

---

* See Appendix A-3 for a demonstration of the optimality of the LOBD and associated conditions; cf., also, Sec. 2.5, above.

where now

$$\ell_j \equiv \ell(x_j) = \left[\frac{d}{dx} \log w_1(x|H_o) \right]_{x=x_j} ; \tag{4.2a}$$

and

$$\hat{B}^*_{n\text{-coh}} = -\frac{1}{2} \sum_i^n L_i^{(2)} \langle a_{oi} s_i \rangle^2 , \quad \text{cf. Eq. (A.1-16).} \tag{4.2b}$$

Similarly, we get

Ia. Coherent Reception (H_2 vs. H_1):

$$g^{(21)}(\underset{\sim}{x})^*_c = [\log \mu_{21} + \hat{B}^{(21)*}_{n\text{-coh}}] - \sum_{j=1}^n [\langle a_{oj}^{(2)} s_j^{(2)} \rangle - \langle a_{oj}^{(1)} s_j^{(1)} \rangle] \ell_j , \tag{4.3}$$

where

$$B^{(2)*}_{n\text{-coh}} = -\frac{1}{2} \sum_i^n L_i^{(2)} \{ \langle a_{oi}^{(2)} s_i^{(2)} \rangle^2 - \langle a_{oi}^{(1)} s_i^{(1)} \rangle^2 \}, \text{ cf. (A.2-45).} \tag{4.3a}$$

[The explicit structures of the various bias terms are derived in Appendix A-1.]

II. Incoherent Reception [H_1 vs. H_o]:

$$g(\underset{\sim}{x})^*_{inc} = [\log \mu + \hat{B}^*_{n\text{-inc}}] + \frac{1}{2!} \sum_{ij}^n [\ell_i \ell_j + \ell_i' \delta_{ij}] \langle a_{oi} a_{oj} s_i s_j \rangle , \tag{4.4}$$

where

$$\hat{B}^*_{n\text{-inc}} = -\frac{1}{8} \sum_{ij}^n \langle a_{oi} a_{oj} s_i s_j \rangle^2 \{ [L_i^{(4)} - 2L_i^{(2)} L_j^{(2)}] \delta_{ij} + 2 L_i^{(2)} L_j^{(2)} \}, \tag{4.4a}$$

cf. (A.1-20a), and

IIa. Incoherent Reception [H_2 vs. H_1]:

$$g^{(2l)}(\underset{\sim}{x})^*_{inc} = [\log \mu_{2l} + \hat{B}^{(2l)*}_{n\text{-}inc}] + \frac{1}{2!} \sum_{ij} (\ell_i \ell_j + \ell'_i \delta_{ij})[\langle (a_{oi} a_{oj} s_i s_j)^{(2)} \rangle$$

$$- \langle (a_{oi} a_{oj} s_i s_j)^{(1)} \rangle] \ , \tag{4.5}$$

where

$$\hat{B}^{(2l)*}_{n\text{-}inc} = - \frac{1}{8} \sum_{ij}^{n} \{\langle a^{(2)}_{oi} a^{(2)}_{oj} s^{(2)}_i s^{(2)}_j \rangle^2 - \langle a^{(1)}_{oi} a^{(1)}_{oj} s^{(1)}_i s^{(1)}_j \rangle^2\}$$

$$\cdot \{(L^{(4)}_i - 2L^{(2)2}_i)\delta_{ij} + 2L^{(2)}_i L^{(2)}_j\}, \tag{4.5a}$$

from (A.2-5ab), and again, the bias terms here are derived in Appendix A-1. The quantity ℓ'_i is

$$\ell'_i = \ell'(x_i) \equiv [\frac{d}{dx} \ell = \frac{d^2}{dx^2} \log w_1(x|H_o)]_{x=x_i} \ ; \text{ with } \delta_{ij}=1, \ i=j; =0, i \neq j \ . \tag{4.6}$$

4.2 Selected Suboptimum Detection Algorithms: (Simple- and Clipper-) Correlation Detectors

We begin with the simple or undistorted coherent (i.e. cross-) correlation detectors, and the corresponding incoherent (or auto-) correlation detectors, which are (threshold) optimum structures when the noise is gaussian [cf. Sec. A.1-3], and which may be optimum at all signal levels when special conditions at the receiver so warrant. [For a discussion of specific examples, see Sec. 20.4-1, [12], Secs. 2.5, 2.6, [20].] For independent noise samples we obtain [from Sec. (2.3), for instance, or Sec. A.1-3):

I. Simple-Correlators:

A. Coherent Reception [H_1 vs. H_0]:

$$g(\underset{\sim}{x})_c = B'_{coh} + \sum_{j=1}^{n} \langle a_{oj} s_j \rangle x_j \ ; \tag{4.7}$$

B. Coherent Reception [H_2 vs. H_1]:

$$g^{(21)}(\underset{\sim}{x})_c = B^{(21)'}_{coh} + \sum_{j=1}^{n} [\langle a_{oj} s_j \rangle^{(2)} - \langle a_{oj} s_j \rangle^{(1)}] x_j \ , \tag{4.8}$$

where the biases are now [cf. A.4-22] specifically

$$B'_{coh} = \log \mu - \frac{1}{2} \sum_{j=1}^{n} \langle a_{oj} s_j{}^2 \rangle ; \ B^{(21)'}_{coh} = \log \mu_{21} - \frac{1}{2} [\sum_{j=1}^{n} \{ \langle (a_{oj} s_j)^{(2)} \rangle^2 - \langle (a_{oj} s_j)^{(1)} \rangle^2 \}] . \tag{4.9}$$

Similarly, for incoherent reception we have

C. Incoherent Reception [H_1 vs. H_0]:

$$g(\underset{\sim}{x})_{inc} = B'_{inc} + \frac{1}{2!} \sum_{ij}^{n} \langle a_{oi} a_{oj} s_i s_j \rangle x_i x_j \ ; \tag{4.10}$$

D. Incoherent Reception [H_2 vs. H_1]:

$$g^{(21)}(\underset{\sim}{x})_{inc} = B^{(21)'}_{inc} + \frac{1}{2!} \sum_{ij}^{n} [\langle (a_{oi} a_{oj} s_i s_j)^{(2)} \rangle - \langle (a_{oi} a_{oj} s_i s_j)^{(1)} \rangle] x_i x_j \ , \tag{4.11}$$

and from [A.4-55] the biases are found to be explicitly

$$B'_{inc} = \log \mu - \frac{1}{2} \sum_{j=1}^{n} \langle (a_{oj} s_j)^2 \rangle - \frac{1}{4} \sum_{ij}^{n} \langle a_{oi} a_{oj} s_i s_j \rangle^2 \tag{4.12a}$$

$$B_{inc}^{(21)'} = \log \mu_{21} - \frac{1}{2}\sum_{j=1}^{n}\{\langle\theta_j^{(2)2}\rangle - \langle\theta_j^{(1)2}\rangle\} - \frac{1}{4}\sum_{ij}^{n}[\langle\theta_i^{(2)}\theta_j^{(2)}\rangle^2$$

$$-\langle\theta_i^{(1)}\theta_j^{(1)}\rangle^2] \ , \ (\theta_j = a_{oj}s_j, \text{ etc.}). \qquad (4.12b)$$

For the energy detector, cf. (A.4-61a), (4.11), (4.12) are simply modified to

(Energy):

$$g^{(21)}(\underset{\sim}{x})_{inc} = B_{inc}^{(21)'} + \frac{1}{2}\sum_{i}^{n}[\langle a_{oi}^2 s_i^2)^{(2)}\rangle - \langle(a_{oi}^2 s_i^2)^{(1)}\rangle]x_i^2 \qquad (4.12b)$$

with the bias

$$B_{inc}^{(21)'} = \log \mu_{21} - \frac{1}{2}\sum_{i}(\langle\theta_i^{(2)2}\rangle - \langle\theta_i^{(1)2}\rangle) - \frac{1}{4}\sum_{i}(\langle\theta_i^{(2)2}\rangle^2\langle\theta_i^{(1)2}\rangle^2) \ , \qquad (4.12c)$$

This shows, as expected, that for detection here, the signal energies must be different, and the larger the difference, the better the discrimination between the (1) and (2) states.

II. Clipper Correlators:

From Secs. A.4-3,4 we may write specifically the (suboptimum) detection algorithms when "super"-clippers are used in the correlation receivers, in contrast to the situation above (I), where there is no distortion. We summarize the results:

A. Coherent Reception [H_1 vs. H_0]:

$$g(\underset{\sim}{x})_{coh} = \log \mu - \sqrt{2}\sum_{i}^{n}\langle\theta_i\rangle^2 w_{1E}(0)_i + \sqrt{2}\sum_{i}^{n}\langle\theta_i\rangle \operatorname{sgn} x_i \ ; \qquad (4.13)$$

B. Coherent Reception [H_2 vs. H_1]:

$$g^{(21)}(\underset{\sim}{x})_c = \log \mu - \sqrt{2} \sum_i^n [\langle \theta_i^{(2)} \rangle^2 - \langle \theta_i^{(1)} \rangle^2] w_{1E}(0)_i + \sum_i^n [\langle \theta_i^{(2)} \rangle - \langle \theta_i^{(1)} \rangle] \text{sgn } x_i . \tag{4.14}$$

Similarly, for the incoherent cases we have

C. Incoherent Reception [H_1 vs. H_0]:

$$g(\underset{\sim}{x})_{inc} = \log \mu - \sum_i^n \langle \theta_i^2 \rangle (1 - \sqrt{2}\, w_{1E}(0)_i) - \frac{1}{4} \sum_{ij}^n \langle \theta_i \theta_j \rangle^2 [8 w_{1E}(0) w_{1E}(0)_j - \{\sqrt{2}\, w''_{1E}(0)_i + 8 w_{1E}(0)_i^2\} \delta_{ij}]$$

$$+ \sum_{ij}^n \langle \theta_i \theta_j \rangle \text{sgn } x_i \text{ sgn } x_j , \tag{4.15}$$

and for binary signals:

D. Incoherent Reception [H_2 vs. H_1]:

$$g^{(21)}(\underset{\sim}{x})_{inc} = \log \mu - \sum_i^n [\langle \theta_i^{(2)^2} \rangle - \langle \theta_i^{(1)^2} \rangle][1 - \sqrt{2}\, w_{1E}(0)_i]$$

$$- \frac{1}{4} \sum_{ij}^n [\langle (\theta_i \theta_j)^{(2)} \rangle^2 - \langle (\theta_i \theta_j)^{(1)} \rangle^2] \{8 w_{1E}(0)_i w_{1E}(0)_j$$

$$- [\sqrt{2}\, w''_{1E}(0)_i + 8 w_{1E}(0)_i^2] \delta_{ij} \} . \tag{4.16}$$

In the above $w_{1E}(0)_i$ is the (jth-) value of the noise pdf (A4-50b) when $x_i = 0$.

4.3 Selected Suboptimum Detection Algorithms: II-Mismatched LOBD's.

Here we indicate "mismatch" by the following device: from (4.1), (4.2) we write

$$\ell_j \to (\ell_{D|E})_j \equiv \frac{d}{dx} \log w_1(x|H_o)_{D|E} \ , \tag{4.17}$$

where D|E denotes D-class parameters, or parameter estimates, D=D', when the pdf of x is chosen (correctly or not) to be E-class. Thus, we have the following varieties of mismatched and matched conditions:

TABLE 4.1. VARIETY OF MISMATCHED AND MATCHED CONDITIONS.

Parameter Values (D)=	Selected Class of Interference (E)=	Remarks
1). D	D	Exact (or "true") parameter values are used in the same postulated class of interference.
(1a). E	E	Same as 1). E≠D, or E = D.)
2). D'	D	Class D estimates, D' (≠D) used in same postulated Class (D) of interference
3). D	E	Class D (exact) parameter values used in chosen Class (E) interference.
4). D'	E	Class D estimates (D'≠D) used in postulated Class E interference

[Interchanging D and E clearly introduces no new forms of relationship. Later, when performance is to be evaluated, along the lines of Sec. 2.4, we shall need to relate the category (E) to the actual, or true, statistical situation, with respect to which the various averages of g*, g, etc. are to be taken, cf. Sec. 6 and Appendix A-I.]

Accordingly, the various possible mismatched threshold detection algorithms follow directly from (4.1)-(4.6) on replacing ℓ_j therein by $\ell_{D|E|j}$, etc., and, correspondingly, g* by the now suboptimum forms $g_{D|E}$, subject to

the combinations of Table 4.1. The bias terms in the LOBD's remain unchanged here. The (generally) suboptimum correlation detectors are not affected by the actual or assumed classes of parameter values or interference statistics.

Finally, in all cases, the complete detection algorithm requires that the number(s) produced by the processing algorithm (g*,g, etc.), as given specifically in Secs. 4.1, 4.2 above, be compared against the appropriate threshold $\log \mathcal{K}$, $\log K$, $\log \mathcal{K}^{(21)}$, cf. (2.2), (2.3), (2.7) respectively: if the threshold is equalled or exceeded, we decide H_1 (or H_2): a signal (or signal 2) is present: if the threshold is not exceeded, we choose the alternative (i.e. null, H_0), or signal 1 cases. We shall give explicit examples in Section 7 ff.

SECTION 5. MATCHED FILTER STRUCTURES: INTERPRETATION OF THE ALGORITHMS

From the earlier analyses of [20], Chapter 4, and the Appendix therein, we can establish matched filter structures for the linear portions of the threshold signal processing explicitly indicated in g,g* for both coherent and incoherent reception cf. (4.1), (4.4), (4.7), (4.10) above. This is important because such structures provide a guide to the actual realization of the physical entities which are needed to carry out the indicated processing, either directly as a computational program, or much more conveniently, usually, by building the specialized mini-computer which represents the operations involved, perhaps in chip form, etc. In the case of specific examples, we shall confine our attention here (in the incoherent cases explicitly) to the important special cases when the desired input signal is narrow-band, the usual situation in telecommunications practice. We consider again the coherent and incoherent cases in detail for the frequently encountered "on-off" (i.e. H_1 vs. H_0) detection situations. Corresponding results for the two-signal (H_2 vs. H_1) are summarized in Sec. 5.

5.1 Coherent Reception (H_1 vs. H_0);

Here we have the situation shown in Figs. 5.1a,b, for both optimum and suboptimum (i.e., cross-correlation detectors). First, in the optimum case, the input sampled data $\{x_j\}$ is non-linearly processed, to yield $y_j=\ell_j$, cf.

(4.1). This new (voltage) sample, [where $y_j=y(t_j)=\ell(x(t_j))$, etc., of course] is then passed through a (linear) "matched filter", where the weighting function of the filter is

$$h_M(T-t_j;T)\Delta t = \langle a_o(t_j)s(t_j)\rangle, \tag{5.1}$$

so that

$$\Psi_n^{(1)*} \equiv \sum_{j=1}^{n} \langle a_{oj}s_i\rangle \ell_j = \sum_{j=1}^{n} y(t_j)h_M(T-t_j;t)\Delta t, \tag{5.2}$$

(which in continuous form becomes, on (0-,T+), the linear functional

$$\Psi_n^{(1)*} \to \Psi_T^{(1)*}(x(t)) = \int_{0-}^{T+} y(t)h_M(T-t,T)dt.) \tag{5.2a}$$

The matched filters are shown in Figs. 5.1a,b. For the suboptimum situation of the cross-correlation detector of (4.7), we have

$$\Psi_n^{(1)} \equiv \sum_{j=1}^{n} \langle a_{oj}s_i\rangle x_j = \sum_{j=1}^{n} x(t_j)h_M(T-t_j;T)\Delta t, \tag{5.2}$$

and all operations here are linear, of course. The matched filter remains the same; only the prefilter processing is different. The filter, h_M, is a form of delay line filter, with suitable weighting ($\sim h_M$) and a read-out at t=T from wherever we choose to start the particular sampling for the interval (t_o,t_o+T), from which we in turn then make the decision indicated by (2.2). We have called such filters "Bayes mached filters of the 1st kind, Type 1", cf. Sec. 4.2, [20], which is, of course, recognized as a special form of (cross-) correlation filter.

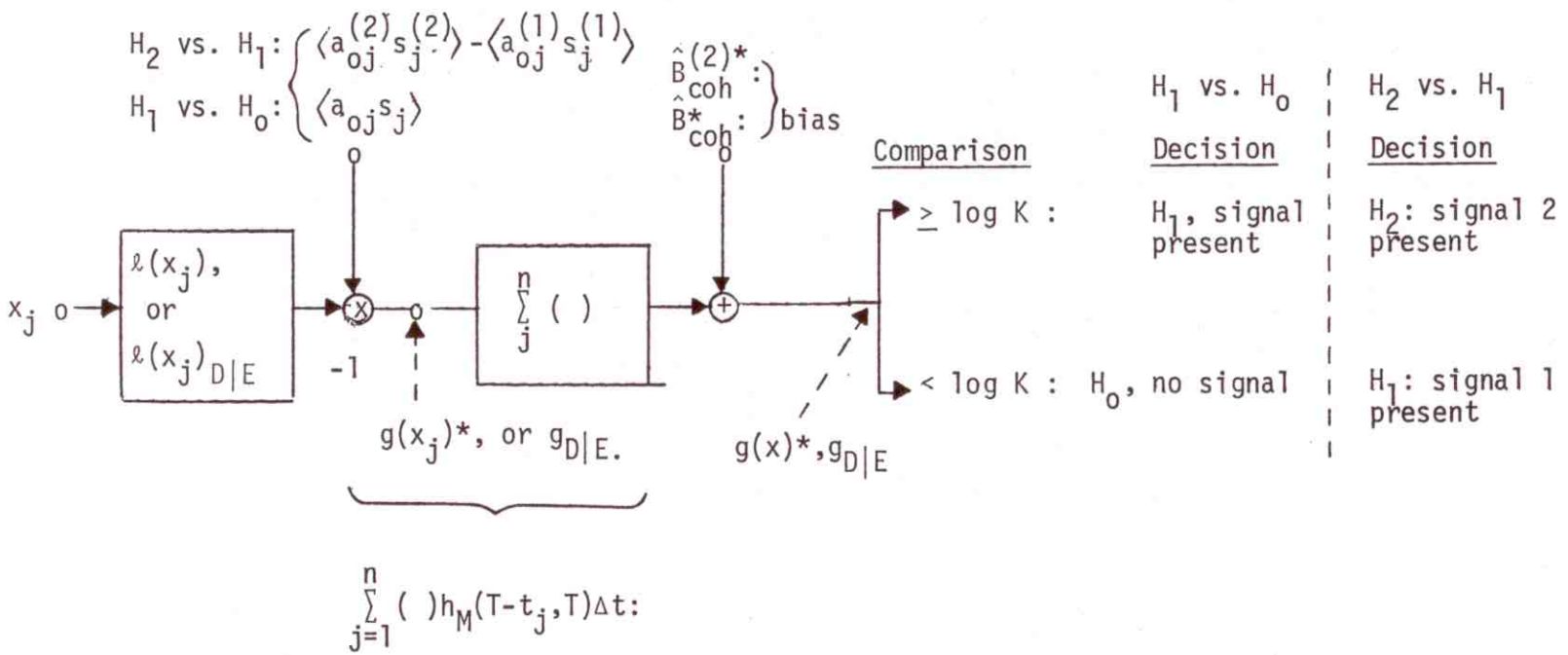

Figure 5.1a LOBD locally optimum threshold receiver, Eq.(4.1), for both "on-off" i.e. (H_1 vs. H_0) and signal 1 vs. signal 2 (H_2 vs. H_1), coherent signal detection, showing matched filter structures [cf. (5.1), (5.2)], [and (4.15), (4.18),[20]]. These are mismatched LOBD's when $\ell \to \ell_{D|E}$, Table 4.1, etc.

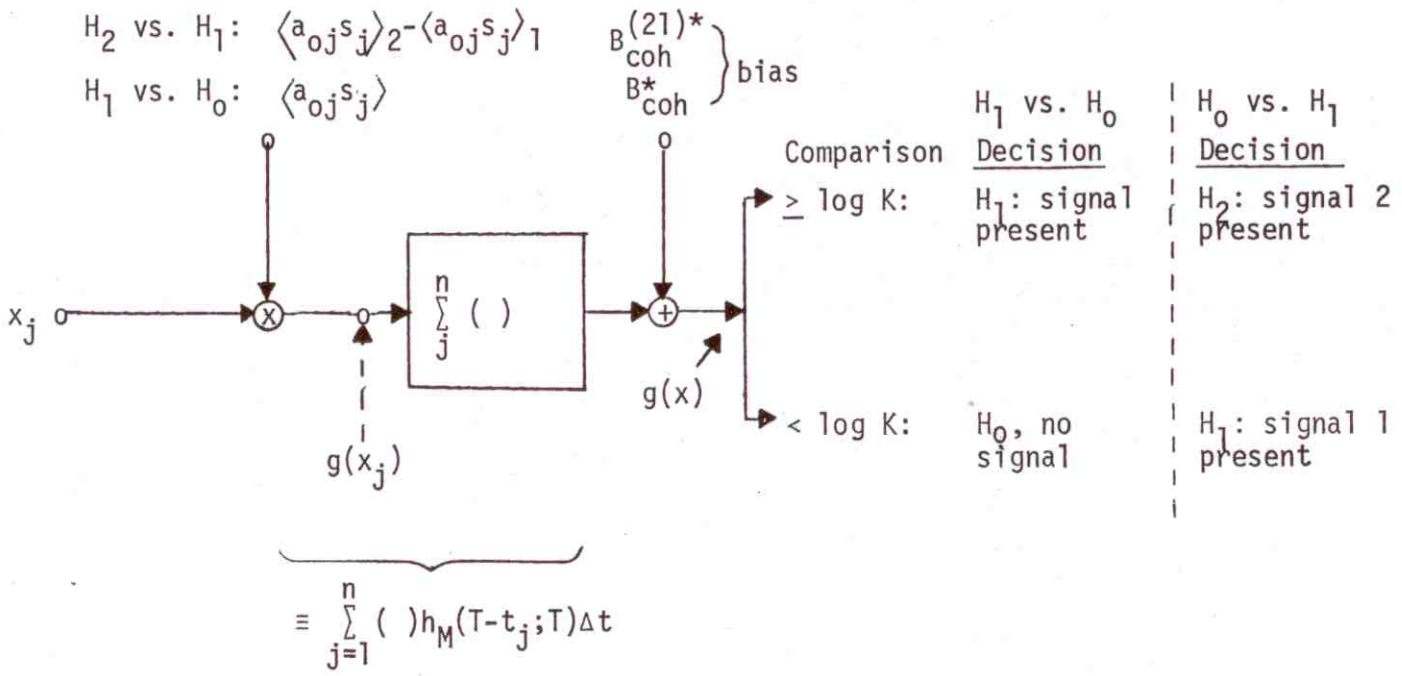

Figure 5.1b (Cross-) correlation detectors, Eq. (4.7), for "on-off" (i.e. H_1 vs. H_o) coherent signal reception showing a matched filter structure (the same as in Fig. 5.1a, cf. Eq. (5.1) et seq.), cf. [20]. Also shown is the binary signal case H_2 vs. H_1, with matched filters, (5.15).

5.2 Incoherent Reception (H_1 vs. H_0):

Here we have the same phenomenon: a highly non-linear operation on the sampled data, to obtain ℓ,ℓ', cf. (4.4), and then to pass these into a second-order nonlinear system, which in this instance can be expressed in the manner of Fig. (5.2), either as a combination of time-varying (linear) filter and zero-memory square-law device, or as another time-varying (linear) filter, and multiplication operation. The point is that the (linear) matched filter here can be represented in two realizable (i.e. operating only on the past) forms. These are:

$$h_M(t_j-t_i,t_j) \equiv \text{sol. of} \begin{cases} \sum_{\ell=1}^{n} h_M(t_\ell-t_i,t_\ell)h_M(t_\ell-t_j,t_\ell)\Delta t=\langle a_{oi}a_{oj}s_is_j\rangle, \\ \qquad\qquad 1 \le i, j \le n \\ = 0, \text{ elsewhere}, \end{cases} \tag{5.4}$$

where

$$\psi^{(2)*} \equiv \sum_{ij}^{n} y_iy_j\langle a_{oi}a_{oj}s_is_j\rangle = \sum_{j=1}^{n} y_j \sum_{i=1}^{(n_2 \text{or } \infty)} y_ih_M(t_j-t_i,t_j)(\Delta t)^2 \tag{5.5}$$

$$= \sum_{j=1}^{n} z(t_i)^2 . \tag{5.5a}$$

The filter, $h_M(t_j-t_i,t_j)$, is time-varying and realizable, and we call it a Bayes matched filter of the 2nd kind, type 1 (cf. Fig. 4.3, [20], also).

In the narrow-band situation we are usually forced to deal with, an equivalent, alternative form of matched filter (e.g. Fig. 5.2, where a multiplier is employed, instead of a zero-memory quadratic device). For this we have

$$\psi^{(2)*} = \sum_{ij}^{n} y_iy_j\hat{h}_M(t_j-t_i,t_j)\Delta t \; ; \quad \hat{h}_M = 0, \; t_i>t_j , \tag{5.6}$$

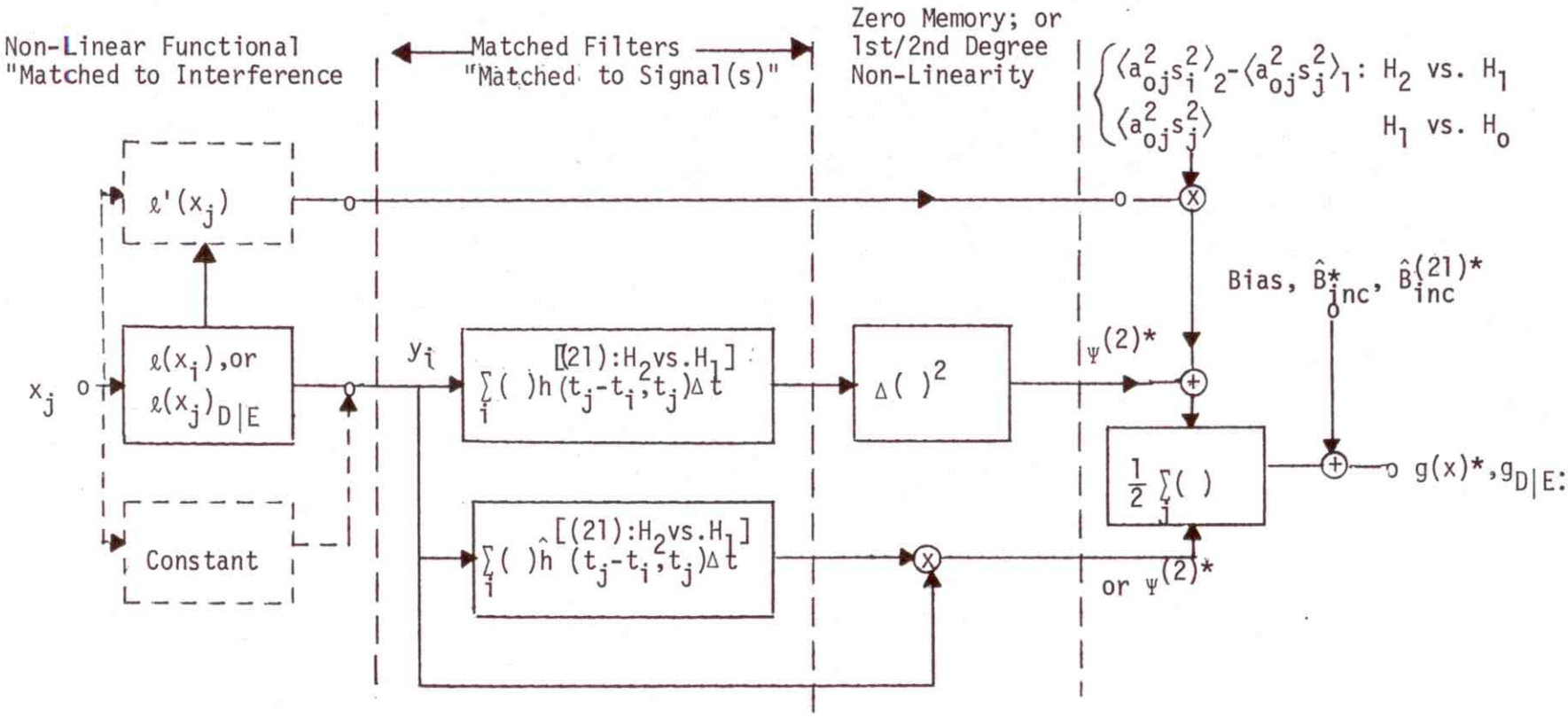

Figure 5.2 LOBD for both optimum, "on-off" (i.e. H_1 vs. H_o) and signal 1 vs. signal 2 (H_2 vs. H_1), incoherent signal detection, Eqs. (4.4), (4.5). [The dotted portion -·-·, applies for the (usually) suboptimum auto-correlation detectors, Eqs. (4.10), (4.11).] The matched filters here, h, $\hat{h}$, (5.4), (5.7) are functionals of the signal auto-correlation functions $a_{oi}a_{oj}s_i s_j$ (1),(2). These are mismatched LOBD's when $\ell \to \ell_{D|E}$, Table 4.1, etc.

where explicitly

$$\hat{h}_M(t_j-t_i,t_j)\Delta t \equiv \left\langle Z_i Z_j^* \right\rangle_\theta \ , \ t_j > t_i; \ =0, \ t_j<t_i \ , \tag{5.7}$$

in which

$$\left\langle Z_i Z_j^* \right\rangle_\theta \equiv \left\langle a_{oi} a_{oj} s_i s_j \right\rangle. \tag{5.7a}$$

This filter is discussed in Sec. 4.3, [20], also, cf. Fig. 4.4, ibid. It is realizable, time-varying, and as in the coherent cases, depends only on the signal statistics; see Sec. 5.3 ff. (The same filter, h_M, or $\hat{h}_M$, clearly applies for the suboptimum, autocorrelator of (4.10), with $y_i \to x_i$, $y_j \to x_j$, a linear transformation, cf. (5.3).)

5.3 Signal Scenarios

Using Sec. 3.1 we can provide a more detailed structure for the above matched filters, including the effects of fading (a) and propagation law (γ), cf. (3.2), (3.2a). Specifically, for narrow band signals without amplitude modulation, we have from (3.2), (3.2a)

$$s_j = \sqrt{2} \cos\left[\omega_o(t_j-\epsilon)-\phi_j-\phi_o\right] \ ; \ a_{oj} = \frac{aG_o}{\lambda^\gamma \sqrt{2\bar{I}_N}} \equiv aB_o \ ; \tag{5.8}$$

$$B_o \equiv G_o/\lambda^\gamma \sqrt{2\bar{I}_N} \ , \tag{5.8a}$$

where the fading effects are governed by the statistics of $\underline{a}$, cf. (3.3), for example.

Thus, for coherent reception the matched filter h_M, (5.1), becomes explicitly

$$h_M(T-t_j,T)\Delta t = a_{oj}\langle s_j\rangle_\epsilon = \bar{a}_{oj}\sqrt{2}\cos\,[\omega_o(t_j-\epsilon_o)-\phi_j-\phi_o],$$

$$0-<t_j<T+;\ =0,\ \text{elsewhere}, \tag{5.9}$$

since $w_1(\epsilon) = \delta(\epsilon-\epsilon_o)$. Moreover, with the assumed stationarity of all random processes here, we have $\bar{a}_{oj} = \bar{a}_o$ $(= \bar{a}\langle B_o\rangle)$, under the further not unreasonable assumption that a_o (and a, B_o) and ϵ are all mutually independent. This result, (5.9), is clearly independent of the fading law, whether or not it is rapid or slow, and whether or not the signal source is moving. This, in turn, is a direct consequence of the coherent mode of detection.

On the other hand, <u>with incoherent reception</u> all the above effects appear explicitly in the structure of the appropriate matched filter [e.g. h_M, $\hat{h}_M$, (5.4), (5.7)], as we might expect, because of the second-order statistics involved. Thus, for example, $\hat{h}_M$, (5.7), becomes now from (5.8)

$$\left.\begin{aligned}\hat{h}_M(t_j-t_i,t_j)\Delta t = \langle a_{oi}a_{oj}\rangle\langle s_i s_j\rangle_{\epsilon,..} &= \langle a_{oi}a_{oj}\rangle\cos[\omega_o(t_i-t_j)-\phi_i+\phi_j],\ t_j>t_i\\ &= 0 \qquad\qquad\qquad\qquad\quad t_j<t_i\end{aligned}\right\}, \tag{5.10}$$

and we have, moreover, the various situations:

(i). <u>slow fading (one-sided):</u>

$$\langle a_{oi}a_{oj}\rangle = \overline{a_o^2} = \overline{a^2}\,\langle G_o^2\rangle/\bar{I}_N\lambda^{2\gamma} \tag{5.11a}$$

(ii). <u>rapid fading (one-sided):</u>

$$\langle a_{oi}a_{oj}\rangle = \overline{a_o^2}\,\delta_{ij} + \bar{a}_o^2(1-\delta_{ij}),$$

$$= \{\overline{a^2}\,\langle G_o^2\rangle/\bar{I}_N\lambda^{2\gamma}\}\delta_{ij}+(1-\delta_{ij})\bar{a}^2\langle G_o\rangle^2/\bar{I}_N\lambda^{2\gamma} \tag{5.11b}$$

(iii). slow fading (two-sided):

$$[\bar{a}_{oj} = 0]; = \overline{a_o^2}\,\delta_{ij} = \overline{a^2}\langle G_o^2\rangle/\bar{I}_N\lambda^{2\gamma}. \tag{5.11c}$$

These results can be extended to include doppler, namely, relative motion between the desired signal source and the receiver: the normalized signal (5.8) is now

$$s_j = \sqrt{2}\cos[(\omega_o+\omega_d)(t_j-\epsilon)-\phi_j-\phi_o] \quad ; \quad \omega_d = \frac{\omega_o v_d}{c_o}\,, \tag{5.12}$$

so that [cf. III, Sec. 5.1 of [34]]

$$\rho_{s\text{-}ij} \equiv \langle s_i s_j\rangle_{\epsilon,\omega_d,\ldots} = e^{-(\Delta\omega_d)^2(t_i-t_j)^2/2}\cos[\omega_o(t_i-t_j)-\phi_i+\phi_j], \tag{5.13}$$

where $\Delta\omega_d = (\omega_o/c_o)\Delta v_d$, $t_i - t_j = (i-j)\Delta T$, and $(\Delta v_d)^2$ is the variance in relative velocity, and we have postulated a gaussian distribution of velocities; c_o is the speed of (wavefront) propagation of EM waves in the medium in question. Applying the relations (5.11) with (5.13) gives, in this more general case,

$$\left.\begin{aligned}\hat{h}_M(t_j-t_i,t_j)\Delta t = \langle a_{oi}a_{oj}\rangle e^{-(\Delta\omega_d)^2(t_i-t_j)^2/2}\cos[\omega_o(t_i-t_j)-\phi_i+\phi_j]\ , \quad & t_j > t_i,\\ = 0\ , \quad & t_j < t_i\end{aligned}\right\} \tag{5.14}$$

for this matched filter for incoherent reception. In this way, from the "anatomy" of the desired signal, from source to receiver, we can construct the desired matched filter for detection. [We remark that still more sophisticated (received) signal forms can be constructed, if the channel itself is dispersive, i.e. has time-delay and frequency spread effects as

well as fading (above), cf. [35]-[38] and remarks at the end of Sec. 3.2 above.]

5.4 Extensions: Binary Signals (H_2 vs. H_1):

The matched filters above for the "on-off" cases (H_1 vs. H_0) are directly modified in the binary signal situation (H_2 vs. H_1). Comparing (4.3), (4.5), (4.8), (4.11) with the respective "on-off" cases, we see at once that (5.1) and (5.7) are modified to

$$h_M^{(21)}{}_{\Delta t}\Big|_{coh} = \langle a_{oj}s_{j2}\rangle - \langle a_{oj}s_j\rangle_1 ; 0 \le t_j \le T; = 0 \text{ elsewhere} ; \tag{5.15a}$$

$$\hat{h}_M^{(21)}{}_{\Delta t}\Big|_{inc} = \langle a_{oi}s_{oj}s_is_j\rangle_2 - \langle a_{oi}a_{oj}s_is_j\rangle_1 , \; t_j > t_i ; = 0 \text{ elsewhere} . \tag{5.15b}$$

From the results of Sec. 5.3 we have, in detail:

$$h_M^{(21)}(T-t_j;T)\Delta T = \sqrt{2}(\langle a_{oj}\rangle_2 \cos[\omega_{o2}(t_j-\epsilon_o)-\phi_j^{(2)}-\phi_o] - \langle a_{oj}\rangle_1 \cos[\omega_{o1}(t_j-\epsilon_o)-\phi_j^{(1)}-\phi_o]) , \tag{5.16}$$

$$0 \le t_j \le T ,$$

for the coherent cases (where any doppler is compensated for). For the incoherent cases (5.14) becomes

$$h_M^{(21)}(t_j-t_i,t_j)\Delta T = e^{-(\Delta\omega_d)^2(t_i-t_j)/2}\{\langle a_{oi}a_{oj}\rangle_2 \cos[\omega_{o2}(t_i-t_j)-\phi_i^{(2)}+\phi_j^{(2)}] - \langle a_{oi}a_{oj}\rangle_1 \cos[\omega_{o1}(t_i-t_j)-\phi_i^{(1)}+\phi_j^{(1)}]\} , \tag{5.17}$$

$$t_j > t_i ; = 0, \; t_i < t_j ,$$

where now the effects of doppler ($\sim \Delta\omega_d$) show up as a common damping factor (since the source of signals 1,2 is the common source). For further "anatomy" of the filter structure, we can use (5.8), (5.8a), for a_{oi}, etc.

5.5 The Generic Character of the LOBD as Adaptive Processor:

At this point it is important to point out a number of general properties of the canonical LOBD's described above. We observe that:

(1). For coherent and incoherent detection - with independent noise samples - the matched filter depends only on signal statistics and structure. Because the LOBD is a threshold system, only first and second-moment statistics of the signal amplitude are needed, Sec. (5.3). [Higher-order statistics are required, of course, for doppler, which is phase variable, cf. (5.13).]

(2). The matched filter (by definition) is always linear, but may or may not be realizable, in the sense of operating only on the "past" of the received data [cf. Chapter 4, [20]);

(3). A variety of equivalent matched filters can be obtained, to represent the data functional $\Psi^{(1)}$, $\Psi^{(2)}$, etc.;

(4). The general functional description of the LOBD is as follows:

(i). It first "matches" the receiver to the (non-gaussian, or gaussian) noise or interference, in that (a), it "adapts" - i.e., determines the Class of interference (A,B, or C) and then estimates the Class parameters, $\mathcal{P}_{3A}$, $\mathcal{P}_{3B}$, etc.- to generate a nongaussian functional, e.g. ℓ,ℓ', of the input data;

(ii). Next, the LOBD then "matches" the signal - as it is a priori known or structured at the receiver - to this new input (ℓ,ℓ', etc.), to form an appropriate correlation detector for the non-gaussian functional ℓ, etc.

These "matched" filters are, by definition, always linear and usually realizable in the causal sense [Sec. 5.2, 5.4];

(iii). For incoherent detection there is an additional, third operation, which follows the matching process, (ii), above. This is usually a nonlinear operation plus summation, where the additional nonlinearity is either a memoryless quadratic process or a multiplication;

(iv). In the mixed cases, of combined coherent and incoherent processing, (usually where there is some RF phase information in narrow-band reception), the nonlinearities following steps (i), (ii), can be more complicated (cf. [1b], Part II, IIC., for example).

Figure 5.3 illustrates the general formalism of LOBD signal detection, for either coherent or incoherent reception, in the prototypical "on-off" case (H_1 vs. H_0). The extension to the binary signal cases (H_2 vs. H_1) is immediate from Sec. 5.4.) Note the key elementsof Locally Optimum Bayes Estimation (LOBD's), of the EMI parameters. (The LOBE theory is developed in parallel concept to that of the LOBD, except that for the most part one operates under the H_1: "signal-present" condition.) The combined operation of LOBD and LOBE is clearly an adaptive process, which, of course, accounts for its usually significant superiority over conventional systems, a priori optimized against gauss noise.

Often, of course, in practice nonoptimum or finite-sample estimates of the parameters of the interfering noise are usually used, as outlined in Sec. 4.3 above. Moreover, before estimating the pertinent noise parameters, it is necessary to establish which class of interference the detector is operating against. One method of doing this is to estimate the pdf (or APD): Class A noise is always distinctively evident by an (almost) zero magnitude of the pdf (or a flat plateau in the APD) between the small-amplitude or "gaussian" region, and the large-amplitude region. In Class B interference there is no zero amplitude region (or flat plateau). [See [6], [7].) An

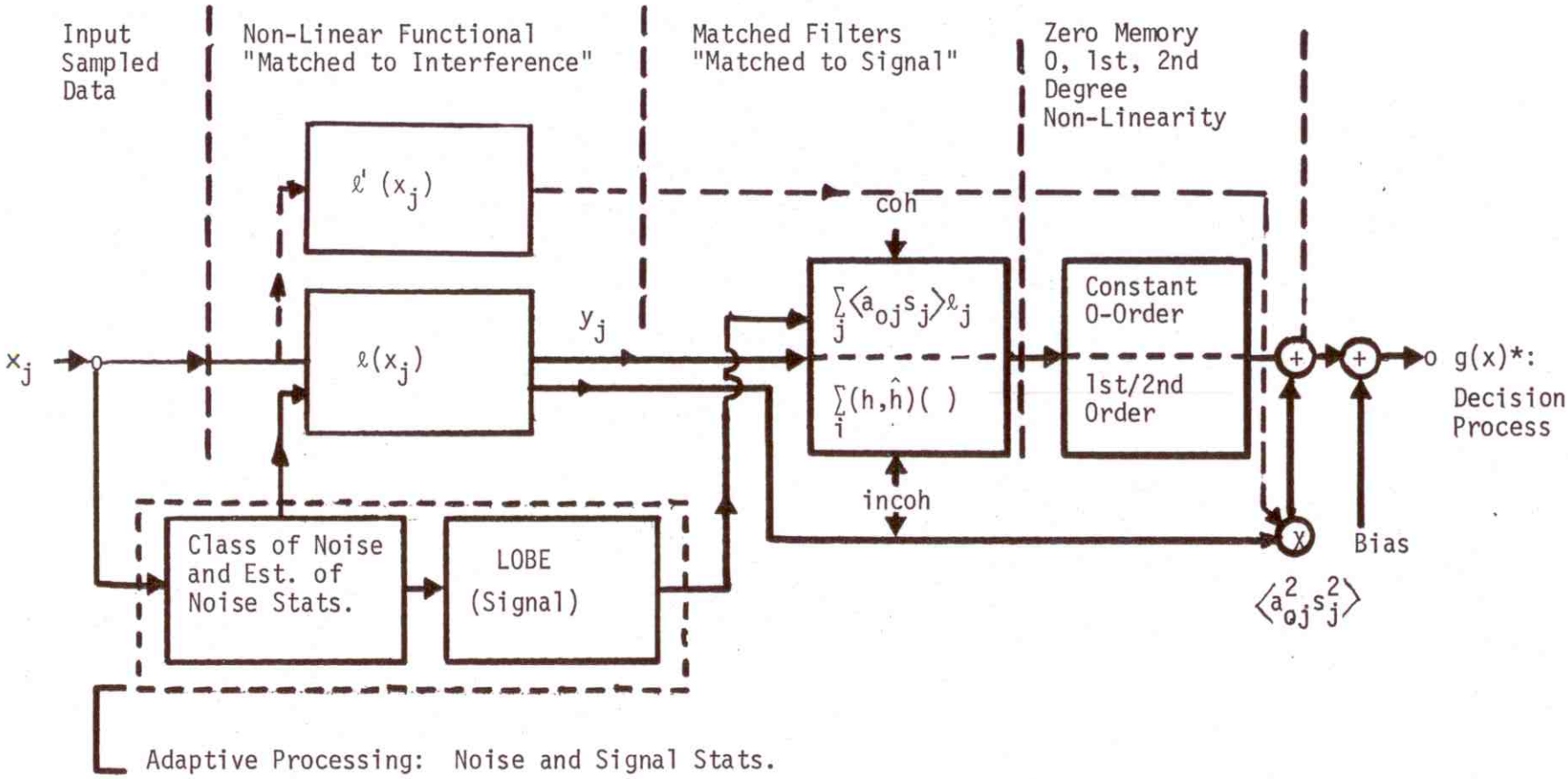

Figure 5.3. The full LOBD for optimum ("on-off", i.e. H_1 vs. H_o) threshold detection of signals in a general EMI environment, for coherent/incoherent reception, and showing the adaptive portion of the optimum receiver [cf. Figs. 5.1, 5.2].

additional advantage of these (estimated) pdf's (etc.) is that they can also be used to give (estimated) values of the Class (A, B) parameters involved, in the manner of [7], for instance. However, if the elements of the EMI scenario are known, the needed parameters can then be calculated, rather than estimated, in the manner of Sec. 3.2 above.

6. PERFORMANCE OF OPTIMUM AND SUBOPTIMUM THRESHOLD DETECTORS: MINIMUM DETECTABLE SIGNALS, PROCESSING GAINS, AND CONDITIONS OF APPLICABILITY

From the general results of Sec. 2.4 and the specific results of Appendices A1-A4, we can obtain at once explicit canonical forms for the various error and correct signal detection probabilities by which performance is most generally measured. This is discussed in Sec. 6.1, while specific structures are reviewed in Sec. 6.2, along with the joint concepts of minimum detectable signal and processing gain, in turn illustrated by the specific relations developed in Appendices A1-A4. In Sections 6.3-6.5 we examine the improvement factors of the optimum detectors over the suboptimum (correlation) detectors discussed in this paper, along with the important conditions on the strength of the input signals which permit us to employ these (analytical) performance measures, and thereby to obtain meaningful numerical results from them. It is shown (in Sec. 6.4), for example, that the set of conditions, for both coherent and incoherent reception, must be simultaneously obeyed, if one is safely to use the performance measures for either mode of reception. This coupling of the coherent and incoherent modes of detection in the evaluation of either mode is the consequence of the fact that coherent detection can never be inferior to incoherent detection under the otherwise same signal and noise conditions of observation. In any case, we emphasize the fact that our results apply generally to all signal types, broad band and narrow band, and can be immediately specialized to narrow band examples as needed, cf. Sec. 7 ff.

We proceed:

6.1 Canonical Performance Measures:

We now apply the specific results of Appendices A1-A4 to Eqs. (2.31)-(2.33), and note that regardless of the mode of detection, optimum (but not suboptimum) algorithms are asymptotically normally distributed, $G(\log \mu \mp \sigma_o^{*2}/2, \sigma_o^{*2})$, where σ_o^{*2} is the variance of the detection algorithm in question (and is the same under both hypotheses).† Here $(\mp)$ refers to: $(-)$, H_o; $(+)$, H_1 in the "on-off" cases, or to H_1, H_2, respectively in the binary signal situations ($s^{(1)}$ vs. $s^{(2)}$). The results are the canonical forms for the correct signal detection probability (Neyman-Pearson Observer) and the error-probability (Ideal Observer), used in ongoing telecommunication reception.

We have, accordingly, since for optimum (threshold) detectors

H_1 vs. H_o:

$$\langle g^* \rangle_1 - \langle g^* \rangle_o = \frac{\sigma_o^{*2}}{2} - (-\frac{\sigma_o^{*2}}{2}) = \sigma_o^{*2};$$

H_2 vs. H_1:

$$\langle g^{(21)^*} \rangle_2 - \langle g^{(21)^*} \rangle_1 = \frac{\sigma_o^{(21)^{*2}}}{2} - (-\frac{\sigma_o^{(21)^{*2}}}{2}) = \sigma_o^{(21)^{*2}} \quad , \qquad (6.1)$$

the relations [from (2.31),(2.32)] for the "on-off" cases, both optimum and suboptimum††

$$\boxed{P_D^{(*)} \doteq \frac{p}{2}\{1+\Theta[\frac{\sigma_o^{(*)}}{\sqrt{2}} - \Theta^{-1}(1-2\alpha_F^{(*)})]\}, \quad \text{(N.P. Observer)}, \qquad (6.2)}$$

where $\alpha_F^{(*)}$ is the false-alarm probability and $\beta_D^{(*)}$ is the false-detection probability††

---

† The suboptimum cases yield asymptotically normal forms, but with different means and variance structures, cf. (6.3) ff.

†† We use the condensed notation $b^{(*)}$ to denote either b* or b, (* ≡ opt.; otherwise suboptimum). It is important to note that the appropriate bias terms (i.e. those for which the algorithms becomes optimum for the corresponding noise [cf. Appendix A4-1,D] are assumed here. Otherwise, one must use (2.31), (2.32) directly. See footnote, next page

$$\alpha_F^{(*)} \doteq \frac{1}{2}\{1-\Theta[\frac{\sigma_o^{(*)}}{2\sqrt{2}} + \frac{\log(\mathcal{K}/\mu)}{\sqrt{2}\,\hat{\sigma}_o}]\};\quad \beta_D^{(*)} \simeq \frac{1}{2}\{1-\Theta[\frac{\sigma_o^{(*)}}{2\sqrt{2}} - \frac{\log(\mathcal{K}/\mu)}{\sqrt{2}\,\hat{\sigma}_o}]\}, \tag{6.3}$$

with

$$\Theta(x) = -\Theta(-x) = \frac{2}{\sqrt{\pi}}\int_0^x e^{-t^2}dt\ ;\quad \Theta^{-1}(y) = x \text{ in } \Theta(x)\ . \tag{6.3a}$$

For the suboptimum cases note the presence of $\hat{\sigma}_o$, (cf. A.4-12,31), as well as σ_o, in the above (and following) expressions. In the optimum cases we have $\sigma_o, \hat{\sigma}_o \to \sigma_o^*$, of course, here†

Similarly, for the Ideal Observer (threshold $\mathcal{K}=1$) in the "on-off" cases, where one considers the error probability $P_e^{(*)} = q\alpha^{(*)}+p\beta^{(*)}$ as the measure of performance, the result here is specifically, on combining (6.3) in $P_e^{(*)}$:

$$P_e^{(*)} \doteq \frac{1}{2}\{1-p\Theta[\frac{\sigma_o^{(*)}}{2\sqrt{2}} - \frac{\log\mu}{\sqrt{2}\,\hat{\sigma}_o^*}]+q\Theta[-\frac{\sigma_o^{(*)}}{2\sqrt{2}} + \frac{\log\mu}{\sqrt{2}\,\hat{\sigma}_o^*}]\},\ \mathcal{K}=1,\ [\text{I.O.}], \tag{6.4}$$

for the general channel ($\mu=p/q\neq 1$, or $\mu=1$). This reduces to the case of the symmetrical channel ($\mu=1$) to the more familiar, simpler result for the optimum cases:†

($\mu=1$):

$$\boxed{P_e^{(*)} \doteq \frac{1}{2}\{1-\Theta[\frac{\sigma_o^{(*)}}{2\sqrt{2}}]\}\ ,\ \mathcal{K}=1,\ [\text{I.O.}].} \tag{6.5}$$

When binary signaling is employed we can also use a Neyman-Pearson Observer (N.P.O.) procedure, where now one of the error probabilities $\alpha_F^{(*)} \to \beta_1^{(2)(*)}$ (the [conditional] probability of incorrectly stating that signal S_2 is present when actually signal S_1 occurs) is preset and the other ($\beta^{(*)} \to \beta_2^{(1)(*)}$ is minimized or otherwise evaluated according to (6.2), which becomes now†

† Our suboptimum cases are here (and subsequently) restricted to those situations where the (nonvanishing) bias is chosen to be the appropriate bias for the class of noise for which these (suboptimum) algorithms, cf. Sec. 4.2, become optimum cf. Appendix A4-1,D. Otherwise, we must employ (2.31),(2.32) directly as performance measures.

$$P_{D-2}^{(*)} \doteq \frac{p_2}{2}\{1+\Theta[\frac{\sigma_o^{(21)(*)}}{\sqrt{2}} - \Theta^{-1}(1-2\beta_1^{(2)(*)})]\}, \qquad \text{[N.P.O.]}, \quad (6.5a)$$

where (6.3) becomes

$$\alpha_F^{(*)} \to \beta_1^{(2)(*)} \doteq \frac{1}{2}\{1-\Theta[\frac{\sigma_o^{(21)*}}{2\sqrt{2}} + \frac{\log(\mathcal{K}^{(21)}/\mu_{21})}{\sqrt{2}\,\hat{\sigma}_o^{(21)(*)}}]\}, \quad \mu_{21}\equiv p_2/p_1, \; p_1+p_2 = 1. \quad (6.5b)$$

$$\beta_D^{(*)} \to \beta_2^{(1)(*)} \doteq \frac{1}{2}\{1-\Theta[\frac{\sigma_o^{(21)*}}{2\sqrt{2}} - \frac{\log(\mathcal{K}^{(21)}/\mu_{21})}{\sqrt{2}\,\hat{\sigma}_o^{(21)(*)}}]\}, \quad (6.5c)$$

and the "on-off" threshold $\mathcal{K}$ is replaced by the binary threshold $\mathcal{K}^{(21)}$. [Clearly, this is symmetrical in S_1, S_2.] Again, note that $\hat{\sigma}_o \neq \sigma_o \neq \sigma_o^*$, cf. (A.4-71-74), and in the optimum cases, $\sigma_o, \hat{\sigma}_o \to \sigma_o^*$. [See footnote, p. 55.]

A more meaningful measure of performance in the binary signal cases, however, is the Ideal Observer [I.O.] above, (6.4), (6.5). Accordingly, from (2.33) and Appendixes A.2-3,4; A.4-3, we find that in these binary threshold cases, canonically, for the "unsymmetric" channel ($\mu_{21}\neq 1$)

$$\underline{(\mu_{21}\neq 1)}: \quad P_e^{(*)} \doteq \frac{1}{2}\{1-p_2\Theta[\frac{\sigma_o^{(21)*}}{2\sqrt{2}} - \frac{\log\mu_{21}}{\sqrt{2}\,\hat{\sigma}_o^{(21)*}}] + p_1\Theta[-\frac{\sigma_o^{(21)*}}{2\sqrt{2}} + \frac{\log\mu_{21}}{\sqrt{2}\,\hat{\sigma}_o^{(21)*}}]\},$$

$$[\text{I.O.}], \mathcal{K}=1 \; . \quad (6.5d)$$

In the more common operational situations it is the symmetric channel ($\mu_{21}=1$) that is used, so that (6.5d) reduces directly to the more familiar, and simpler, threshold result:

$$\underline{(\mu_{21}=1)}: \quad P_e^{(*)} \doteq \frac{1}{2}\{1-\Theta[\frac{\sigma_o^{(21)(*)}}{2\sqrt{2}}]\}, \; [\text{I.O.}, \mathcal{K}=\mu_{21}=1]. \quad (6.5e)$$

This, like (6.2)-(6.5d) above, is a canonical form; [but note the restriction, footnote, p. 55.]

Finally, as we have noted earlier and recall now, various conditions on the "smallness" of the input signals ($\wedge a_o^2 > 0$) must be satisfied if these performance measures (6.2)-(6.5e) are to predict receiver performance accurately. These conditions will be discussed in Sec. 6.4 ff. In the meantime, we note that these results above are canonical in several ways: (i), their form is independent of the mode (coherent or incoherent) of reception; (ii), they are independent, formally, of signal structure, (i.e. narrow-band as well as broad-band signal are included), and (iii), last but by no means least, they are likewise invariant, formally, for the explicit noise statistics.

6.2 Minimum Detectable Signals and Processing Gains:†

We can "anatomize" the quantities $[\sigma_o^{(*)2}, \sigma_o^{(2l)(*)2}]$, identifying the "minimum detectable signal" and "processing gain" through the following definition of "output signal-to-noise ratio" when the (total) noise is stationary:

$$\boxed{\left(\frac{S}{N}\right)_{out}^{(*)2} \equiv \frac{\sigma_o^{(*)2}}{2} \equiv \Pi^{(*)}(n) f^{(*)}(\langle a_o^2\rangle_{min}^{(*)}) = \Pi^{(*)}(n) f^{(*)}\left[\left(\frac{S}{N}\right)_{in\text{-}min}^{2(*)}\right],} \quad (6.6)$$

where $\Pi^{(*)}(n)$ is the processing gain, and $\langle a_o^2\rangle_{min}^{(*)}$ is the minimum input detectable signal (-to-noise ratio), $\left(\frac{S}{N}\right)_{in\text{-}min}^{2(*)}$, or more loosely, the minimum detectable signal. Here, $f^{(*)}(\langle a_o^2\rangle_{min}^{(*)})$ is some (simple) power of $\langle a_o^2\rangle_{min}^{(*)}$, as we shall note below, cf. (6.9), (6.22b), whose structure depends on the mode of observation. The quantity $(S/N)_{out}^{(*)2}$ is an effective output signal-to-noise (intensity) ratio, after processing, which determines the performance of the detector in these threshold regimes, according to the appropriate probability measures, (6.2), (6.4), (6.5) above. The minimum detectable input signal-to-noise ratio $\langle a_o^2\rangle_{min}^{(*)}$ has its component signal and noise intensities measured at the same point in the receiver, usually at the output of the receiver's (linear) front-end stages, before subsequent nonlinear processing (as exhibited in the algorithms $g_n^{(*)}(\underset{\sim}{x})$, etc.). The minimum detectable signal is the least (normalized) input signal (intensity) which

---

See footnotes on pp. 54, and p. 55, particularly.

can be sensed at the receiver, subject to the particular controls of the decision probabilities and observation time (i.e. sample-size, n).

From the assumption of "practical optimality" discussed in Sec. 2.4 above, where it is sufficient that the H_1-variance, $(\sigma^*_{in})^2$, of the threshold algorithm be effectively equal to the H_o-variance, $(\sigma^*_{on})^2$, e.g.

$$\therefore \begin{cases} (\sigma^*_{in})^2 = (\sigma^*_{on})^2 + F(n,\overline{a_o^2}) \doteq (\sigma^*_{on})^2 \ , \quad n >> 1, \\ F(n,\overline{a_o^2}) << (\sigma^*_{on})^2 \ , \end{cases}$$

cf. (2.29), we can also derive the useful concept of "minimum detectable signal", $\langle a_o^2\rangle^*_{min}$, and associated processing gain, Π^*. This is because the condition $F(n,\overline{a_o^2})/(\sigma^*_{on})^2 << 1$, establishing a maximum value for threshold signals, $\langle a_o^2\rangle$, for which the algorithms are still LO and AO, cf. Appendix A3, also establishes a non-vanishing input signal-to-noise ratio, $\langle a_o^2\rangle^*$, for all n, and particularly, large n, such that $0 < \langle a_o^2\rangle^*_{min} \leq [\langle a_o^2\rangle^*_{min}]_{max} (<<1)$, where $[\langle a_o^2\rangle^*_{min}]_{max}$ is determined by our selection of the quantitative meaning of "<<" in the above condition. This is physically consistent with our notion of input signal, which is, of course, always nonvanishing.

Accordingly, instead of minimum detectable signal we can equally well ask for the corresponding maximum detectable range, $r^{(*)}_{d\text{-}max}$, of the desired signal. This is obtained in Sec. 3.1 from (3.1), (3.2) and the definition

$$\langle a_o^2\rangle^{(*)}_{min} \equiv \langle I_S\rangle / \langle I_N\rangle = \left(\frac{S}{N}\right)^2_{TR} \frac{1}{(r^{(*)}_{d\text{-}max})^{2\gamma}} \ ;$$

$$\left(\frac{S}{N}\right)^2_{TR} = \frac{\overline{a^2}(\langle \hat{I}_o^2\rangle/2)^{1/2}}{\langle I_N\rangle} = \frac{\overline{a^2}(\overline{G_o^2}/2)(c_o/\hat{r}_o)^{2\gamma}}{\Omega_2 + \sigma_G^2} \ , \qquad (6.7)$$

which incorporates the various elements of the propagation law, interference scenario (Sec. 3.2), fading, beam-pattern structure of desired source and receiver, etc. Thus, $(S/N)^2_{TR}$, in contrast to $(S/N)^2_{out}$ in (6.6), is a signal-to-noise intensity ratio which is a measure of the desired signal level

at the transmitter output, in terms of the noise or interference level at the output of the (linear) front-end stages of the receiver. From (6.6), (6.7) we see that $r^{(*)}_{d\text{-}max}$ may be obtained from the relation

$$r^{(*)}_{d\text{-}max} = [(\frac{S}{N})^2_{TR}/\langle a_o^2\rangle^{(*)}_{min}]^{1/2\gamma} = \{(\frac{S}{N})^2_{TR}/f^{-1}(\sigma_o^{(*)2}/2\Pi^{(*)})\}^{1/2\gamma} , \qquad (6.8)$$

so that once $\langle a_o^2\rangle^{(*)}_{min}$, or $\sigma_o^{(*)}$ and $\Pi^{(*)}$ are specified, along with the function f, maximum detectable range can be calculated, as well. This has been done in a recent study by Middleton [34], and will not be pursued further in the present investigation.

In order to determine $\Pi^{(*)}$ and $a_o^{2\ (*)}_{\ min}$ in (6.6) we need the specific results of Appendices 2, 4. We begin with

I. Optimum Coherent Threshold Detection:

From (A.2-14), in (6.6) we have (for henceforth stationary noise processes):†

$$\sigma^{*2}_{o\text{-}coh} = 2\Pi^*_{coh}\langle a_o^2\rangle^*_{min\text{-}coh} = 2(nL^{(2)})\ (\frac{1}{2n}\sum_i^n \langle a_{oi}s_i\rangle^2), \text{ Eq. (A.2-14).} \qquad (6.9)$$

$$\therefore \quad \boxed{\Pi^*_{coh} = nL^{(2)}\ ;\ \langle a_o^2\rangle^*_{min\text{-}coh} = \frac{1}{2n}\sum_i^n \langle a_o s_i\rangle^2} , \qquad (6.10)$$

with

$$L^{(2)} \equiv \langle \ell^2\rangle_o = \int_{-\infty}^{\infty} \{\frac{d}{dx} \log w_1(x|H_o)\}^2 w_1(x|H_o)dx ,$$

$$= \int_{-\infty}^{\infty} (w_1'/w_1)^2 w_1(x|H_o)dx, \text{ Eq. (A.1-15),} \qquad (6.10a)$$

---

† See footnote, p. 102.

and f*( ) in (6.6) is clearly ( )^1, i.e., the first power of the indicated argument. Noting that here the sampling process may be adjusted for narrow-band signals so that $\langle s_i \rangle = s_{max} = \sqrt{2}$ and with no real restriction as to generality in regarding $\underline{a}$ and $\underline{s}$ to be statistically independent, so that $\langle a_o s_i \rangle = \overline{a_o}\sqrt{2}$, we see that $\langle a_o^2 \rangle^*_{min\text{-}coh} = \bar{a}_o^2$: regardless of the fading law, only the mean amplitude is relevant. [This is not the case for the maximum range, however, where both $\overline{a_o}$ and a_o^2 ($\sim\overline{a^2}$) are required, cf. (6.7).] We also obtain, on solving (6.2), or (6.5), for σ_o^*, and then using (6.9), the following useful expression for the minimum detectable signal:

$$\langle a_o^2 \rangle^*_{min\text{-}coh} = (\Pi^*_{coh})^{-1} \begin{cases} \Theta^{-1}(2p_D^*-1)+\Theta^{-1}(1-2\alpha_F^*) \\ 2\Theta^{-1}(1-2P_e^*) \end{cases}^2 \begin{matrix} :[N.P.O.],\ p_D^* \equiv P_D^*/p. \\ :[I.O.]:\mu=1. \end{matrix} \qquad (6.11)$$

$$= (\Pi^*_{coh})^{-1}\{C^{(*)2}_{N.P.} \text{ or } C^{(*)2}_{I.O.}\}, \qquad (6.11a)$$

with

$$C^*_{N.P.} = \sqrt{B^*_{N.P.}} \equiv \Theta^{-1}(2p_D^*-1)+\Theta^{-1}(1-2\alpha_F^*) \ ; \ C^*_{I.O.} \equiv 2\Theta^{-1}(1-2P_e^*) \equiv \sqrt{B^*_{I.O.}} \qquad (6.11b)$$

This relation shows how the minimum detectable signal depends on sample size and the background noise (via Π^*) and on the "controls" in detection, e.g. p_D^*, α_F^*, P_e^*.

For binary signals we use (A.2-50a) in (6.6), to get in these stationary cases

<u>binary:</u> $(\sigma^{(2l)*}_{o\text{-}coh})^2 = 2\Pi^{(2l)*}_{coh}\langle a_o^2 \rangle^{(2l)*}_{min\text{-}coh}$

$$\equiv 2(nL^{(2)})\left(\frac{1}{2n}\sum_i^n (\langle a^{(2)}_{oi} s^{(2)}_i \rangle - \langle a^{(1)}_{oi} s^{(1)}_i \rangle)^2\right), \text{ Eq. (A.2-50a)}, \qquad (6.12)$$

so that

$$\therefore \quad \boxed{\Pi_{coh}^{(21)*} = nL^{(2)};\ \langle a_o^2\rangle_{min\text{-}coh}^{(21)*} \equiv \frac{1}{2n}\sum_i^n \left(\overline{a_{oi}^{(2)}}\langle s_i^{(2)}\rangle - \overline{a_{oi}^{(1)}}\langle s_i^{(1)}\rangle\right)^2.} \tag{6.13}$$

We have also, cf. (6.11a), the equivalent expression

$$\langle a_o^2\rangle_{min\text{-}coh}^{(21)*} = (\Pi_{coh}^{(21)*})^{-1}\{C_{N.P.}^{(*)2} \text{ or } C_{I.O.}^{(*)2}\}^2 . \tag{6.13a}$$

With equal amplitudes ($a_o^{(2)} = a_o^{(1)}$), a usual condition of operation, the effective minimum detectable signal becomes now

$$\langle a_o^2\rangle_{min\text{-}coh}^{(21)*} \equiv \bar{a}_o^2 \cdot \sum_i^n \left(\frac{\langle s_i^{(2)}\rangle - \langle s_i^{(1)}\rangle}{\sqrt{2n}}\right)^2 . \tag{6.14}$$

By inspection, it as once evident that choosing <u>antipodal signals</u>, e.g. $s_i^{(1)} = -s_i^{(2)}$, and selecting the t_i such that $s_i = s_{max} = \sqrt{2}$ (at least for narrow-band signals) maximizes the minimum detectable signal here [as well as $\sigma_o^{(21)*}$], and hence further minimizes P_e^*. Thus, from (6.14) we have

<u>antipodal:</u> $\quad \langle a_o^2\rangle_{min\text{-}coh}^{(21)*} = 4\bar{a}_o^2 .$ (6.15a)

Similarly, for <u>orthogonal signals</u>, e.g.

$$s_i^{(2)} = \sqrt{2}\cos\omega_o t_i \ ; \quad s_i^{(1)} = \sqrt{2}\sin\omega_o t_i \ , \tag{6.15b}$$

we see that the sum in (6.14) becomes

$$\langle a_o^2\rangle^{(21)*}_{\text{min-coh}} = \frac{\bar{a}_o^2}{n}\sum_i^n (\cos\omega_o t_i - \sin\omega_o t_i)^2 = \bar{a}_o^2\{1 - \frac{1}{n}\sum_i^n \sin(\omega_o t_i/2)\},$$

$$= 2\bar{a}_o^2 \text{ , (orthogonal),} \qquad (6.15b)$$

which is thus maximized by choosing the sampling times $t_i = k(4i-1)\pi/\omega_o$, where $k/\omega_o = 1/2\pi B = T/2\pi$, in which B is the bandwidth of the signals, which are "on" during (t_o, t_o+T) intervals. Of course, for "on-off" signalling, $s_i^{(1)}=0$ here and $\langle a_o^2\rangle^{(21)*}_{\text{min-coh}} \to \langle a_o^2\rangle^*_{\text{min-coh}} = \bar{a}_o^2$, cf. (6.10) et seq. Accordingly, we have obtained quite readily the well-known results that for the same total signal intensity, binary antipodal signals are superior to binary orthogonal signals, and are equivalent to "on-off" operation (this last, since $\bar{a}_o|_{\text{binary}} \to 2\bar{a}_o|_{\text{on-off}}$ under the same power conditions). By "superior" here is meant smaller error probabilities (or larger P_D's, cf. (6.2)), since $\sigma_o^{(21)*}$ is increased in the antipodal cases vis-à-vis the orthogonal signals.

II. Suboptimum Coherent Threshold Detection (Cross-Correlators)

From (A.4-52a) we obtain in the case of the suboptimum cross-correlators for "on-off" operation in the usual stationary régimes:

$$\sigma^2_{o\text{-coh}} \equiv 2\Pi_{\text{coh}}\langle a_o^2\rangle_{\text{min-coh}} = 2(n)(\sum_i^n \langle a_o s_i\rangle^2/2n) \qquad (6.16)$$

$$\therefore\ \Pi_{\text{coh}} = n\ ;\ \langle a_o^2\rangle_{\text{min-coh}} = \frac{\bar{a}_o^2}{2n}\sum_{i=1}^n \langle s_i\rangle^2 \to \bar{a}_o^2\ . \qquad (6.17)$$

Comparing (6.17) and (6.10) we see at once that here

$$\boxed{\Pi_{\text{coh}}/\Pi^*_{\text{coh}} \equiv \Phi^*_{\text{d-coh}} = L^{(2)^{-1}}(\leq 1)} \text{ , where } L^{(2)} = \text{Eq. (6.10a).} \qquad (6.18)$$

The quantity $\Phi^*_{\text{d-coh}}$ is the degradation factor for these cross-correlation detectors (4.7) vis-à-vis the optimum (threshold) detector (4.1), for the

same input signals, observation periods (n), and coherent (mode of) observation. Thus, $\Phi^*_{d\text{-coh}}$ is, not unexpectedly, determined by the statistical character of the noise alone, through $L^{(2)}$, (6.10a). For gauss noise $L^{(2)} = 1$, cf. A.1-3, but for the usually encountered non-gaussian noise, $L^{(2)} >> 1$. [See Sec. 8 for various values of $L^{(2)}$, etc.]

With binary signals we use (A.4-20) to write similarly

$$\sigma^{(21)^2}_{o\text{-coh}} \equiv 2\Pi^{(21)}_{coh}\langle a_o^2\rangle^{(21)}_{min\text{-}coh} = 2\cdot(n)\cdot\{\sum_i^n \left(\frac{\langle a_o^{(2)}s_i^{(2)}\rangle - \langle a_o^{(1)}s_i^{(1)}\rangle}{\sqrt{2n}}\right)^2\}\ ; \tag{6.19}$$

$$\therefore\ \Pi^{(21)}_{coh} = n;\quad \langle a_o^2\rangle^{(21)}_{min\text{-}coh} = \bar{a}_o^2 \sum_{i=1}^n \left(\frac{\langle s_i^{(2)}\rangle - \langle s_i^{(1)}\rangle}{\sqrt{2n}}\right)^2 , \tag{6.20}$$

(with $a_o^{(2)} = a_o^{(1)}$, usually), and, again, the degradation factor becomes

$$\Pi^{(21)}_{coh}/\Pi^{(21)*}_{coh} \equiv \Phi^{(21)*}_{d\text{-coh}} = 1/L^{(2)} , \tag{6.21}$$

unchanged from the "on-off" cases above. Similarly, expressions like (6.11), (6.13) for the minimum detectable signal in these suboptimum cases are

$$\langle a_o^2\rangle_{min\text{-}coh} = \Pi^{-1}_{coh}\{C^2_{N.P.} \text{ or } C^2_{I.O.}\}\ ;\ \langle a_o^2\rangle^{(21)}_{min\text{-}coh} = \Pi^{(21)^{-1}}_{coh}\{C^2_{N.P.} \text{ or } C^2_{I.O.}\} , \tag{6.21a}$$

where $C_{N.P.} = \Theta^{-1}(2p_D-1)+\Theta^{-1}(1-2\alpha_F)$, etc. are the <u>suboptimum versions</u> of the controls for the N.P. and I.O. cases, e.g. $p_D^* \to p_D$, $P_e^* \to P_e$, Sec. 6.1.

<u>III. Optimum Incoherent Threshold Detection:</u>

We proceed as above for the coherent cases. Here we apply (A.2-40) to obtain for "on-off" signalling (in the stationary régime):

"on-off": $$\sigma^{*2}_{o\text{-inc}} = \frac{1}{4}\sum_{ij}^{n}\langle a_{oi}a_{oj}s_is_j\rangle^2\{(L^{(4)}-2L^{(2)^2})\delta_{ij}+2L^{(2)^2}\} \tag{6.22a}$$

$$\equiv 2\Pi^*_{inc}(\langle a_o^2\rangle^*_{min\text{-}inc})^2 , \tag{6.22b}$$

so that

$$\boxed{\langle a_o^2\rangle^*_{min\text{-}inc} \equiv \{\frac{1}{2}\sum_{i}^{n}\langle a_{oi}^2 s_i^2\rangle\}^{1/2} \to (\frac{1}{2}\sum_{i}^{n}\overline{a_o^2}) = \overline{a_o^2}} \tag{6.23}$$

$(\overline{s_i^2} = 1$, by normalization).

Accordingly, applying (6.23) to (6.22a,b) gives directly the processing gain for these incoherent, "on-off" threshold signal detectors:

$$\boxed{\Pi^*_{inc} = \frac{nL^{(4)}}{8}\{1+\frac{2L^{(2)^2}}{L^{(4)}}(Q_n-1)\},} \tag{6.24}$$

where

$$\boxed{Q_n-1 \equiv \frac{1}{n}\sum_{ij}^{n}{}' m_{ij}^2\rho_{ij}^2 \ (\geq 0)} \ ; \ m_{ij} \equiv \langle a_{oi}a_{oj}\rangle/\overline{a_o^2} \ ; \ \rho_{ij} \equiv \langle s_is_j\rangle. \tag{6.25}$$

Here $L^{(2)}$ has been specified in (6.10a), while $L^{(4)}$, cf. (A.1-19b), is given by

$$L^{(4)} = \langle(\ell^2+\ell')^2\rangle_o = \int_{-\infty}^{\infty}(\frac{w_1''}{w_1})^2 w_1(x|H_o)dx \tag{6.26}$$

and is also expressed numerically in Sec. 7. We now observe that the processing gain (6.24) depends on signal structure, as well as on sample size (n) and noise statistics, unlike the coherent cases, cf. (6.10).

The minimum detectable signal (6.23) may also be written, by (6.22b) in (6.2) or (6.5), as

$$\langle a_o^2\rangle^*_{\text{min-inc}} = (\Pi^*_{\text{inc}})^{-1/2}\left\{\begin{array}{l}\Theta^{-1}(2p_D^*-1)+\Theta^{-1}(1-2\alpha_F^*)\\ 2\Theta^{-1}(1-2P_e^*)\end{array}\right\}\begin{array}{l}:\text{ N.P.O.}\\:\text{ I.O.}\end{array} \quad ,p_D^*\equiv P^*_{D/P}, \tag{6.27}$$

$$= (\Pi^*_{\text{inc}})^{-1/2}\{C^*_{\text{N.P.}} \text{ or } C^*_{\text{I.O.}}\}\ , \tag{6.27a}$$

cf. (6.11): note the different exponents on Π^* and $\{\Theta^{-1}\ldots\}$, etc.

For binary signals we next use (A.2-56) with (A.2-52a), to write (in these stationary régimes)

binary:

$$(\sigma^{(21)*}_{o\text{-inc}})^2 \equiv 2\Pi^{(21)*}_{\text{inc}}(\langle a_o^2\rangle^{(21)*}_{\text{min-inc}})^2 = \frac{1}{4}\sum_{ij}^{n}(\langle a^{(2)}_{oi}a^{(2)}_{oj}s^{(2)}_i s^{(2)}_j\rangle - \langle a^{(1)}_{oi}a^{(1)}_{oj}s^{(1)}_i s^{(1)}_j\rangle)^2$$
$$\cdot\{(L^{(4)}-2L^{(2)^2})\delta_{ij}+2L^{(2)^2}\} \ , \tag{6.28}$$

so that, parallelling (6.22a)-(6.25) we get in these binary cases the following expresssions for the minimum detectable signal and associated processing gain $[\langle a_o^{(2)^2}\rangle \neq \langle a_o^{(1)^2}\rangle]$:

$$\langle a_o^2\rangle^{(21)*}_{\text{min-inc}} \equiv \{\frac{1}{n}\sum_{i}^{n}(\langle(a_o^{(2)}s_i^{(2)})^2\rangle - \langle(a_o^{(1)}s_i^{(1)})^2\rangle)^2\}^{1/2}$$
$$= \langle a_o^{(2)^2}\rangle - \langle a_o^{(1)^2}\rangle, \ (\neq 0), \tag{6.29}$$

since $\langle (s_i^{(2),(1)})^2 \rangle = 1$ by normalization, and

$$\Pi_{inc}^{(21)*} = \frac{nL^{(4)}}{8}\{1 + \frac{2L^{(2)^2}}{L^{(4)}}[Q_n^{(21)}-1]\}, \tag{6.30}$$

where specifically

$$Q_n^{(21)}-1 \equiv \sum_{ij}{}' \frac{\{\langle a_{oi}^{(2)}a_{oj}^{(2)}\rangle \rho_{ij}^{(2s)} - \langle a_{oi}^{(1)}a_{oj}^{(1)}\rangle \rho_{ij}^{(1s)}\}^2}{n\{\langle a_o^{(2)}\rangle^2 - \langle a_o^{(1)}\rangle^2\}^2} \; ; \; \rho_{ij}^{(\ )} \equiv \langle s_i^{(\ )} s_j^{(\ )}\rangle . \tag{6.31}$$

$$= \sum_{ij}{}' \frac{\{\langle a_o^{(2)}\rangle^2 m_{ij}^{(2)} \rho_{ij}^{(2s)} - \langle a_o^{(1)}\rangle^2 m_{ij}^{(1)} \rho_{ij}^{(1s)}\}^2}{n\{\langle a_o^{(2)}\rangle^2 - \langle a_o^{(1)^2}\rangle\}^2} \tag{6.31a}$$

where we have used the definition of m_{ij} in (6.25) above.

In the important special cases where the signal amplitudes are equal, $a_o^{(2)} = a_o^{(1)} = a_o$, e.g. $\langle a_o^{(2)^2}\rangle = \langle a_o^{(1)^2}\rangle = \langle a_o^2\rangle$ ($\neq 0$), (6.28) simplifies to

$\underline{a_o^{(1)} = a_o^{(2)}}$:

$$(\sigma_{o\text{-}inc}^{(21)*})^2 = 2\Pi_{inc}^{(21)*}\langle a_o^2\rangle_{inc}^{(21)*} = \frac{\overline{a_o^2}^2 L^{(2)^2}}{2} \sum_{ij}{}' m_{ij}^2(\rho_{ij}^{(2s)} - \rho_{ij}^{(1s)})^2 , \tag{6.32}$$

so that

$\underline{a_o^{(1)} = a_o^{(2)}}$:

$$\langle a_o^2\rangle_{min\text{-}inc}^{(21)*} = \overline{a_o^2}; \; \therefore \Pi_{inc}^{(21)*} = \frac{n^2 L^{(2)^2}}{4} \sum_{ij}{}' \frac{m_{ij}^2(\rho_{ij}^{(2s)} - \rho_{ij}^{(1s)})^2}{n^2} \equiv \frac{nL^{(2)^2}}{4}(\hat{Q}_n^{(21)}-1) \tag{6.33}$$

which defines $\hat{Q}_n^{(21)}$, e.g.

$$\boxed{\hat{Q}_n^{(21)}{}_{-1} \equiv \sum_{ij}^{n} \frac{m_{ij}^2(\rho_{ij}^{(2s)}-\rho_{ij}^{(1s)})^2}{n}} \quad . \tag{6.33a}$$

In all instances we have the binary analogue of (6.27), viz:

$$\langle a_o^2\rangle_{\text{min-inc}}^{(21)*} = (\Pi_{\text{inc}}^{(21)*})^{-1/2}\{C_{\text{N.P.}}^{*} \text{ or } C_{\text{I.O.}}^{*}\} \quad . \tag{6.34}$$

IV. Suboptimum Incoherent Threshold Detection (Auto-correlators):

From (A.4-58b) we now obtain for "on-off" signalling and stationary régimes when the (generally suboptimum) auto-correlators (A.4-56) are used:

$$\sigma_{\text{o-inc}}^2 \equiv 2\Pi_{\text{inc}}\langle a_o^2\rangle_{\text{min-inc}}^2 = (\sum_{ij}^{n}\langle a_{oi}a_{oj}s_is_j\rangle^2)^2 / \sum_{ij}^{n}\langle a_{oi}a_{oj}s_is_j\rangle^2 \cdot[(\overline{x^4}-3)\delta_{ij}+2] \quad , \tag{6.35}$$

cf. (6.22), so that

$$\langle a_o^2\rangle_{\text{min-inc}} \equiv \{\frac{1}{n}\sum_i\langle a_o^2\rangle^2\langle s_i^2\rangle^2\}^{1/2} = \overline{a_o^2} \quad , \text{ cf. (6.23)} \quad , \tag{6.36a}$$

and

$$\therefore \quad \Pi_{\text{inc}}|_{\text{correl}} = \frac{n^2\left(\sum_{ij}^{n}\frac{m_{ij}^2\rho_{ij}^2}{n}\right)^2}{2\sum_{ij}m_{ij}^2\rho_{ij}^2[(\overline{x^4}-3)\delta_{ij}+2]} = \frac{nQ_n^2}{2[(\overline{x^4}-1)+2(Q_n-1)]} \tag{6.36b}$$

for the minimum detectable signal and processing gain for these auto-correlation detectors. Analogous to (6.27) we have

$$\langle a_o^2 \rangle_{\text{min-inc}} = \Pi_{\text{inc}}^{-1/2} \begin{cases} \Theta^{-1}(2p_D-1)+\Theta^{-1}(1-2\alpha_F) \\ 2\Theta^{-1}(1-2P_e) \end{cases} \begin{matrix} :\underline{\text{N.P.}} \\ :\underline{\text{I.O.}} \end{matrix} = \Pi_{\text{inc}}^{-1/2}\{C_{\text{N.P.}} \text{ or } C_{\text{I.O.}}\} , \tag{6.37}$$

where again $C_{N.P.}$, etc. is the suboptimum version of the control $C^*_{N.P.}$, etc., (6.27).

Comparing (6.36b) with (6.24) gives us the <u>degradation factor</u> for these (simple) correlators in nongaussian noise

<u>"on-off":</u>

$$\boxed{\Phi^*_{\text{d-inc}} \equiv \Pi_{\text{inc}}/\Pi^*_{\text{inc}} = 4Q_n^2/[\overline{x^4}-1+2(Q_n-1)][L^{(4)}+2L^{(2)^2}(Q_n-1)]} , \tag{6.38}$$

where $L^{(2)}$, $L^{(4)}$ are given by (6.10a), (6.26) respectively. As expected, when the noise is gaussian, $L^{(2)} = 1$, $L^{(4)} = 2$, and $\therefore \Phi_{\text{d-inc}} = 1$: the (simpler) autocorrelator is itself threshold optimum now. Unlike the coherent cases, however, cf. (6.18), $\Phi_{\text{d-inc}}$ depends on signal structure and sample size (n), as well as on the noise statistics, $L^{(2)}$, $L^{(4)}$.

With binary signals we use (A.4-72b) in these (stationary) suboptimum incoherent situations, to write similarly, cf. (6.35):

<u>binary:</u>

$$\sigma^{(21)^2}_{\text{o-inc}} = \frac{(\sum_{ij}^{n} \{\langle (a_{oi}a_{oj}s_is_j)^{(2)}\rangle - \langle (a_{oi}a_{oj}s_is_j)^{(1)}\rangle\}^2)^2}{\sum_{ij}^{n} \{\langle (a_{oi}a_{oj}s_is_j)^{(2)}\rangle - \langle (a_{oi}a_{oj}s_is_j)^{(1)}\rangle\}^2[(\overline{x^4}-3)\delta_{ij}+2]} \tag{6.39a}$$

$$\equiv 2\Pi^{(21)}_{\text{inc}}(\langle a_o^2\rangle^{(21)}_{\text{min-inc}})^2 , \tag{6.39b}$$

and paralleling (6.29)-(6.31) we have

$$\langle a_o^2\rangle^{(21)}_{\text{min-inc}} = \langle a_o^{(2)^2}\rangle - \langle a_o^{(1)^2}\rangle \neq 0 \; ; \qquad \boxed{\Pi^{(21)}_{\text{inc}} = \frac{nQ_n^{(21)^2}}{2[(\overline{x^4}-1)+2(Q_n^{(21)}-1)]}} \; , \tag{6.40}$$

where $Q_n^{(21)}$, $a_o^{(2)} \neq a_o^{(1)}$, is given by (6.31). However, for the important situations where $a_o^{(2)} = a_o^{(1)} = a_o$, the above simplify to

$\underline{a_o^{(2)} = a_o^{(1)}:}$

$$\langle a_o^2\rangle^{(21)}_{\text{min-inc}} = \overline{a_o^2} \; ; \qquad \boxed{\Pi^{(21)}_{\text{inc}} = \frac{n(\hat{Q}_n^{(21)}-1)^2}{2[\overline{x^4}-1+2(\hat{Q}_n^{(21)}-1)]}} \; , \tag{6.41}$$

and $Q_n^{(21)}$, (6.31), is now replaced by $\hat{Q}_n^{(21)}$, (6.33a); $\langle a_o^2\rangle^{(21)}_{\text{min-inc}}$ is also given by (6.34), where $C^*_{\text{N.P.}} \to C_{\text{N.P.}}$; etc., cf. (6.21a) et seq.

Finally, the <u>degradation factor</u> $\Phi^{(21)}_{\text{d-inc}}$ becomes from (6.30) and (6.40) $[a_o^{(2)} \neq a_o^{(1)}]$, and (6.33) and (6.41), $[a_o^{(2)} = a_o^{(1)}]$:

$$\Phi^{(21)*}_{\text{d-inc}}(n)\big| \equiv \Pi^{(21)}_{\text{inc}}/\Pi^{(21)*}_{\text{inc}} = \begin{cases} \dfrac{4Q_n^{(21)^2}}{[\overline{x^4}-1+2(Q_n^{(21)}-1)][L^{(4)}+2L^{(2)^2}(Q_n^{(21)}-1)]} : \\ \qquad\qquad a_o^{(2)} \neq a_o^{(1)} \qquad (6.42a) \\ \dfrac{2(\hat{Q}_n^{(21)}-1)}{[\overline{x^4}-1+2(\hat{Q}_n^{(21)}-1)]L^{(2)^2}} \; ; \; a_o^{(2)} = a_o^{(1)} \; , \\ \qquad\qquad (6.42b) \end{cases}$$

which reduce for gaussian noise ($\overline{x^4}=3$), to unity, as expected. Equations

(6.42a,b) are to be contrasted with $\Phi_d^{(21)*} = 1/L^{(2)}$, (6.21). Like the "on-off" cases, the degradation factor also depends on the noise statistics, on sample size, and signal structure. Finally, note that (6.34) applies in this suboptimum situation:

$$\langle a_o^2 \rangle_{\text{min-inc}}^{(21)} = (\Pi_{\text{inc}}^{(21)})^{-1/2} (C_{\text{N.P.}} \text{ or } C_{\text{I.O.}}). \tag{6.37}$$

It is convenient to sumarize the various results of this section 6.2 in the following two Tables: The Notes to Table 6.1a apply equally to Table 6.1b, 6.2 ff. Note that the results analogous to those shown in the text and summarized in Tables 6.1a,b, and for the clipper correlators Sec. A.4-3, are provided in Table 6.2.